Quasiparticle trapping in quench dynamics of superconductor/quantum dot/superconductor Josephson junctions

Jingjing Cheng,[1] Xueying Zuo,[1] Jian Wang,[2,3] and Yanxia Xing[1,*]

[1]*Key Laboratory of Advanced Optoelectronic Quantum Architecture and Measurement, Ministry of Education, Beijing Institute of Technology, Beijing 10081, China*

[2]*College of Physics and Optoelectronic Engineering, Shenzhen University, Shenzhen 518060, China*

[3]*Department of Physics, The University of Hong Kong, Pokfulam Road, Hong Kong, China*

(Received 6 June 2024; revised 18 August 2024; accepted 21 August 2024; published 12 September 2024)

With the aid of Keldysh nonequilibrium Green's functions, we investigate the quench dynamics in a superconductor–quantum dot–superconductor (S-QD-S) Josephson junction during transient transport processes going beyond the wide-band limit. We calculate the transient current when the bias is suddenly turned off/on. We find that because of the distinct physical mechanisms that govern superconducting current in zero-bias and nonzero-bias scenarios, the quench dynamics of the "turning-off" and "turning-on" transient processes exhibit significant differences. When the bias is turned off, aided by quasiparticle bound states, electrons become trapped in the energy gap and oscillate between the bound states $\pm\epsilon_b$. Consequently, the turning-off transient current exhibits oscillations at a frequency of $2\epsilon_b$, which is dependent on ϕ. Because the bound states in a ϕ-driven Josephson junction have an infinite lifetime, the turning-off transient current exhibits perpetual oscillations and relaxes towards the steady state at an infinitely slow rate. In contrast, the turning-on transient current, which is underpinned by multiple Andreev reflections, quickly settles into a steady alternating state at a frequency of $2V$. The infinite relaxation time of the turning-off transient current, in conjunction with the distinct quench dynamics observed during both "turning-off" and "turning-on" operations, reveals the unique role of quasiparticle trapping in superconducting transient transport processes.

DOI: 10.1103/PhysRevB.110.125417

I. INTRODUCTION

The growing demand for smaller and faster quantum devices has spurred extensive experimental [1] and theoretical [2] research into quantum transport through mesoscopic junctions over the past few decades. Taking the form of an S-QD-S structure, where a normal quantum dot is sandwiched between two superconducting layers, the Josephson junctions exemplifies an interacting open quantum system. These junctions provide an ideal platform for a variety of quantum devices, including superconducting quantum interference devices (SQUIDs) [3], Cooper pair splitters [4,5], superconducting spin qubits [6–8], topological superconducting quantum bits [9,10], quasiparticle detectors [11], and single-electron sources [12]. Within the superconducting gap, single-electron excitations are prohibited. Instead, an electron with energy above the Fermi level that enters the system can only be reflected as a hole with energy below the Fermi level. This phenomenon is known as Andreev reflection (AR) [13]. When a voltage bias is applied [14–16], multiple Andreev reflections (MARs) enable a single electron to be scattered out of the superconducting gap, as depicted in Fig. 1(a). This results in an alternating current with a frequency of $2V$, where V is defined as the difference between the left V_L and right V_R voltages. Conversely, in the absence of a voltage bias [17,18], AR remains confined within the superconducting gap. This confinement results in single electrons becoming trapped in the quantum dot, thereby facilitating the formation of Andreev bound states (ABSs) [19,20], as shown in Fig. 1(b). These ABSs support a direct supercurrent that is modulated by the superconducting phase difference ϕ and exhibits a $\sin(\phi)$-like behavior. In transient transport, a step-like bias connects two distinct steady states: one driven by the superconducting phase difference ϕ and the other by the voltage drop V. Given the significant differences in the physical origins and mathematical representations of supercurrents between zero-bias and nonzero-bias conditions, it is expected that the quench dynamics of the transient processes will exhibit unique features that distinguish them from those found in conventional systems.

Transient transport holds paramount importance, both in fundamental research and practical applications [10,21–30]. Central to this field is the response speed, a critical parameter that quantifies the swiftness with which a device achieves a steady state upon the sudden "turning-on/off" of a bias. Transient transport has been extensively studied through various theoretical approaches. These include nonequilibrium Green's functions [21,22,24], iterative solutions to the time-dependent Schrödinger equation [23,26], master equation [29], full counting statistics [27,28,31,32], and complex absorbing potentials [33]. Additionally, researchers have employed the time-dependent numerical renormalization group [34–36], continuous-time quantum Monte Carlo simulations [37,38], time-dependent density-functional theory [39,40], the

*Contact author: xingyanxia@bit.edu.cn

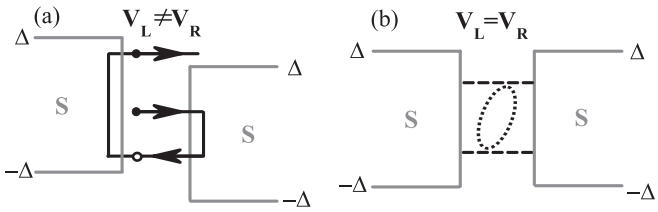

FIG. 1. (a) In the presence of voltage bias $V = V_L - V_R$, the single electrons are scattered out of superconducting gap through MARs. (b) When bias is closed, electrons are trapped in the quantum dot, and oscillate between two bound states $\pm\epsilon_b$.

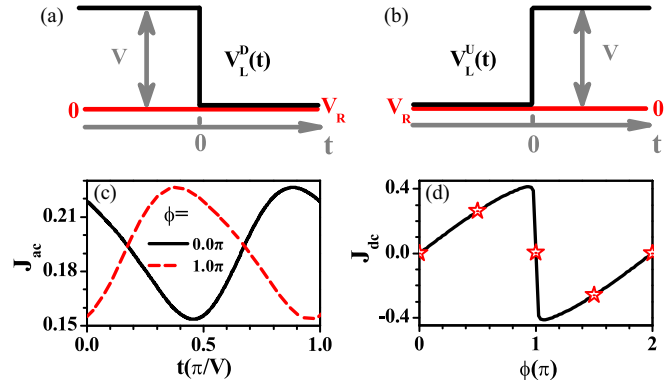

FIG. 2. (a), (b) Schematic diagram of downwards and upwards step-like bias. (c), (d) ac and dc current in remote past (future) for downwards (upwards) and upwards (downwards) case. Parameters: dc bias $V = 0.8$, line width function $\Gamma = 0.8$.

continuous unitary transformation technique [41,42], and self-consistent perturbative theory [36,43]. These methods prove to be highly effective for dealing with simple systems, such as those suitable for the wide-band approximation and systems capable of quantum tunneling. However, when it comes to the S-QD-S Josephson junction, the wide-band limit becomes inapplicable due to the influence of superconducting leads, and in the zero-bias scenario, only bound states are present. This poses a significant challenge to the existing methods. Therefore, until now, no studies have been conducted on the transient processes of S-QD-S Josephson junctions. Now, we resort to a solution that can address bound states and extend beyond the wide-band limit.

In this paper, by precisely solving the time-dependent Dyson equation [21,24,25], we derive an accurate transient current solution going beyond wide-band limit, which, in turn, demands substantial computational resources. By analyzing the mathematical properties of steady-state nonequilibrium Green's functions (NEGF), we significantly mitigate the substantial computational cost through analytical methods. To solve the time-dependent Dyson equation, the Hamiltonian of the nonequilibrium system can be decomposed into an unperturbed component and a time-dependent component. There are two principal methods for this division. The first method is known as the "partitioned approach" [44–47], where the isolated quantum dot and leads constitute the unperturbed part. The coupling between the central region and the leads is adiabatically introduced at $t = 0$. While the "partitioned approach" offers computational convenience, it is impractical for transient transport due to the difficulty of instantaneously controlling the coupling between the central region and the leads. Therefore, we opt for an alternative scheme, the "partition-free approach" [48]. In this approach, the central region is perpetually connected to the external leads, extending back into the distant past. At $t = 0$, a time-dependent external bias is introduced to the system. Subsequently, the unperturbed component is defined as the nonequilibrium steady state in the remote future ($t \to \infty$). The perturbation caused by the time-dependent bias is then treated as an interaction, which can be characterized by a time-dependent self-energy.

In this paper, transient transport is driven by a step-like bias $V(t)$. We consider two distinct step-like biases: a downwards and upwards step, with the bias being turned off/on at $t = 0$, respectively, as depicted in Figs. 2(a) and 2(b). The "turn-on/off" operation connects the transition between two steady states: the remote past state and the final future state. After an abrupt voltage change, the steady current, which originated in the past state, evolves and gradually approaches the characteristics of its final future state. Acknowledging the fundamental irreversibility inherent in time, the "turn-on" process cannot be considered a mere inversion of the "turn-off" process [24,25]. In the case of the S-QD-S Josephson junction, the transient process exhibits increased complexity and remarkable characteristics. In the downwards case, when the voltage bias is turned off, MARs from the remote steady state rapidly diminish. Concurrently, ABSs with infinite lifetimes become dominant. The step-like bias stimulates transitions between two ABSs at $\pm\epsilon_b$. As a result, the "turning-off" transient current oscillates at a frequency of $2|\epsilon_b|$ and approaches its final state asymptotically. In contrast, the "turning-on" transient current, facilitated by MARs with their finite lifetimes, swiftly achieves a steady alternating state with a characterized frequency of $2V$. The infinite relaxation time of the "turning-off" transient current, in conjunction with the distinctly contrasting quench dynamics observed during abrupt "turning-on" and "turning-off" events, reveals the unique role of quasiparticle trapping in superconducting transient transport processes. It provides significant insights into the experimental identification of intrinsic properties of quantum system, as well as the observation of quasiparticle trapping phenomena within junction materials.

The structure of the remainder of this paper is as follows: Section II introduces the time-dependent Hamiltonian within the mean-field BCS theory, represented in Nambu space, and presents the general formulas and rigorous solutions for the "turning-off" and "turning-on" transient currents $J^D(t)$ and $J^U(t)$. Section III contains the numerical results and in-depth physical discussions. A concise summary is presented in Sec. IV, complemented by additional technical details in Appendices A and B.

II. HAMILTONIAN AND FORMULA

In this section, we introduce the microscopic model of the S-QD-S Josephson junction and derive the analytical expressions for the transient current that result from a sudden voltage drop or lift.

A. Time-dependent Hamiltonian

We examine a model Hamiltonian of an S-QD-S Josephson junction, where a single-level quantum dot is connected to distinct Fermi reservoirs through left and right superconducting leads. The Fermi levels of these electron reservoirs are controlled by the respective voltages V_α, where α denotes either the left (L) or right (R) lead. The voltages V_L and V_R may be identical, resulting in a zero bias, or they may differ, leading to a nonzero bias V. The Hamiltonian for the system is generally expressed as

$$H(t) = \sum_\alpha H_\alpha(t) + H_c(t) + H_t.$$

This Hamiltonian is composed of the Hamiltonian for the isolated central quantum dot $H_c(t)$, the Hamiltonians for the two superconducting terminal leads $H_\alpha(t)$ with $\alpha = L, R$, and the tunnel-coupled term H_t between central region and superconducting leads. In our analysis of transient transport, the voltage V_α is considered time dependent, which consequently renders the superconducting lead Hamiltonian H_α time dependent as well. Owing to the long-range Coulomb interaction, it is necessary to account for the internal potential $U(t)$ that is influenced by $V_\alpha(t)$ [49]. This consideration implies that the central quantum dot Hamiltonian H_c also exhibits time dependence. Furthermore, we adopt the "partition-free approach", under which the tunneling Hamiltonian H_t is treated as time independent.

Then, the individual Hamiltonians are formally expressed as follows:

$$\begin{aligned}
H_\alpha(t) &= \sum_{k_\alpha,\sigma} \epsilon_{k_\alpha}(t) c^\dagger_{k_\alpha,\sigma} c_{k_\alpha,\sigma} \\
&\quad + \sum_k \tilde{\Delta}_\alpha(t) c^\dagger_{-k_\alpha,\uparrow} c^\dagger_{k_\alpha,\downarrow} + \tilde{\Delta}^*_\alpha(t) c_{k_\alpha,\downarrow} c_{-k_\alpha,\uparrow}, \\
H_c(t) &= \sum_\sigma \epsilon_d(t) d^\dagger_\sigma d_\sigma, \\
H_t &= \sum_{k_\alpha,\sigma} t_{k_\alpha,\sigma} c^\dagger_{k_\alpha,\sigma} d_\sigma + t^*_{k_\alpha,\sigma} d^\dagger_\sigma c_{k_\alpha,\sigma},
\end{aligned} \tag{1}$$

where $c^\dagger_{k_\alpha,\sigma}$ and $c_{k_\alpha,\sigma}$ are the creation and annihilation operators for electrons in the αth superconducting lead, respectively, with σ denoting spin and k representing momentum. The operators $d^\dagger_\sigma$ and d_σ are the creation and annihilation operators for the quantum dot. The coefficient $t_{k_\alpha,\sigma}$ characterizes the tunneling strength between the quantum dot and the αth superconducting lead. Within the mean-field approximation, the many-body interactions in the superconductor are included within the pair potential. This approximation results in a complex superconducting order parameter given by $\tilde{\Delta}_\alpha = \Delta_\alpha e^{i\phi_\alpha}$, where Δ_α represents the modulus and ϕ_α denotes the phase of the complex order parameter. Under zero-voltage conditions, the single-electron energy $\epsilon^0_{k_\alpha,\sigma}$ and the superconducting order parameter $\tilde{\Delta}_\alpha$ are considered constant. However, upon application of a time-dependent voltage $V_\alpha(t)$, the single-electron energy experiences a shift, described by $\epsilon_{k_\alpha,\sigma}(t) = \epsilon^0_{k_\alpha,\sigma} + eV_\alpha(t)$ [50,51]. Concurrently, the superconducting order parameter evolves in response to the voltage as $\tilde{\Delta}_\alpha(t) = \tilde{\Delta}_\alpha e^{-\frac{2i}{\hbar}\int_0^t eV_\alpha(\tau)d\tau}$ [52]. The influence of $V_\alpha(t)$ extends to the quantum dot, where the energy level ϵ_0 is altered according to $\epsilon_d(t) = \epsilon_0 + U(t)$. This shift is attributed to the Coulomb interactions between the leads and the quantum dot. The linear internal potential $U(t)$ is expressed as $U(t) = -e\sum_\alpha u_\alpha V_\alpha(t)$, with u_α being the characteristic potentials that fulfill $\sum_\alpha u_\alpha = 1$ to ensure gauge invariance of the long-range Coulomb interaction [53]. The characteristic potentials u_α are defined as $u_\alpha = \Gamma_\alpha / \sum_\alpha \Gamma_\alpha$, representing the relative strength of the coupling between the quantum dot and the superconducting leads, ensuring both simplicity and physical plausibility.

To facilitate numerical calculations, we implement a unitary transformation to the Hamiltonian (1),

$$P(t) = \exp\left[\sum_{k_\alpha,\sigma}\left(i\frac{\phi_\alpha}{2} + i\frac{e}{\hbar}\int_0^t d\tau V_\alpha(\tau) c^\dagger_{k_\alpha,\sigma} c_{k_\alpha,\sigma}\right)\right],$$

where for notational simplicity, we henceforth set the elementary charge e and the reduced Planck constant $\hbar$ to unity, $e = \hbar = 1$. Under this transformation, the time dependence of $H_\alpha(t)$ and the superconducting phases ϕ_α are effectively transferred to the coupling terms $t_{k_\alpha,\sigma}$ within the Hamiltonian H_t. For convenience, and considering that the Fermi energy of the lead is aligned with the superconductor condensate, we set the Fermi energy to zero. Consequently, positive energy states are associated with spin-up electrons, while negative energy states correspond to spin-down holes. We introduce the Nambu spinor field operators as follows [54]:

$$\mathbf{\Psi}_{k_\alpha} = \begin{pmatrix} c_{k_\alpha,\uparrow} \\ c^\dagger_{-k_\alpha,\downarrow} \end{pmatrix}, \quad \mathbf{\Phi}_d = \begin{pmatrix} d_\uparrow \\ d^\dagger_\downarrow \end{pmatrix},$$

which allows us to express the transformed Hamiltonian $\tilde{H}(t)$ in a compact 2×2 Nambu representation,

$$\tilde{H}_\alpha = \sum_k \mathbf{\Psi}^\dagger_{k_\alpha} \begin{pmatrix} \epsilon^0_{k_\alpha} & \Delta_\alpha \\ \Delta_\alpha & -\epsilon^0_{-k_\alpha} \end{pmatrix} \mathbf{\Psi}_{k_\alpha},$$

$$\tilde{H}_c(t) = \mathbf{\Phi}^\dagger_d \begin{pmatrix} \epsilon_d(t) & \\ & -\epsilon_d(t) \end{pmatrix} \mathbf{\Phi}_d,$$

$$\tilde{H}_t(t) = \sum_{k_\alpha} \mathbf{\Psi}^\dagger_{k_\alpha} \mathbf{T}_{k_\alpha}(t) \mathbf{\Phi}_d + \text{H.c.},$$

where $\mathbf{T}_{k_\alpha}(t) = \mathbf{T}^0_{k_\alpha} \mathbf{W}_\alpha(t)$, and

$$\mathbf{T}^0_{k_\alpha} = \begin{pmatrix} t_{k_\alpha,\uparrow} e^{i\phi_\alpha/2} & 0 \\ 0 & -t^*_{k_\alpha,\downarrow} e^{-i\phi_\alpha/2} \end{pmatrix},$$

$$\mathbf{W}_\alpha(t) = \begin{pmatrix} e^{i\int_0^t d\tau V_\alpha(\tau)} & 0 \\ 0 & e^{-i\int_0^t d\tau V_\alpha(\tau)} \end{pmatrix}.$$

The transient current in our system is driven by the time-dependent voltage difference $V(t) = V_L(t) - V_R(t)$. For simplicity, we set the right lead voltage $V_R(t)$ to zero, which implies $\mathbf{W}_R(t) = \mathbf{I}$, the identity matrix. Consequently, the time-dependent bias reduces to $V(t) = V_L(t)$. In our calculations, we consider two types of voltage biases to simulate the

voltage turning-off and turning-on processes,

$$V_L^D(t)=\begin{cases}V, & t<0,\\ 0, & t\geqslant 0,\end{cases}\quad\text{and}\quad V_L^U(t)=\begin{cases}0, & t<0,\\ V, & t\geqslant 0,\end{cases}$$

respectively. To ensures that the time-dependent history is only included in the period before $t=0$, we define a modified time-dependent voltage $\tilde{V}_L(t)$ that is zero for $t>0$,

$$\tilde{V}(t)=V\theta(t)=\begin{cases}V, & t<0,\\ 0, & t\geqslant 0,\end{cases}$$

and write $V(t)$ as $V_L^D(t)=\tilde{V}(t)$ and $V_L^U(t)=V-\tilde{V}(t)$. The corresponding transformation matrices for the downwards and upwards step-like biases are given by

$$\mathbf{W}_L^D(t)=\tilde{\mathbf{W}}(t),\quad \mathbf{W}_L^U(t)=\bar{\mathbf{W}}(t)\tilde{\mathbf{W}}^\dagger(t),$$

where

$$\bar{\mathbf{W}}(t)=\begin{pmatrix}e^{iVt} & 0\\ 0 & e^{-iVt}\end{pmatrix},\quad \tilde{\mathbf{W}}(t)=\begin{pmatrix}e^{i\int_0^t d\tau\tilde{V}(\tau)} & 0\\ 0 & e^{-i\int_0^t d\tau\tilde{V}(\tau)}\end{pmatrix}.$$

B. $J_\alpha^{\rm in}(t)$ and $J_\alpha^{\rm out}(t)$

The current operator $\hat{J}_\alpha$ is generally derived from the time evolution of the particle number operator of the αth superconducting lead [50],

$$\hat{J}_\alpha=-\frac{d\hat{N}_\alpha}{dt}=i\left[\sum_k \mathbf{\Psi}_{k_\alpha}^\dagger\sigma_z\mathbf{\Psi}_{k_\alpha},\hat{H}\right],$$

where the Pauli matrix σ_z is introduced to distinguish between electrons and holes within the framework of the Nambu representation. Considering current conservation, the net conduction current is defined as $J=\frac{1}{2}(J_L-J_R)$. We will now proceed to derive J_α for $\alpha=L,R$. Taking the expectation value over the equilibrium quantum state, we obtain the superconducting current

$$\begin{aligned}J_\alpha(t)&=i\sum_k\left\langle\mathbf{\Psi}_{k_\alpha}^\dagger\sigma_z\mathbf{T}_{k_\alpha}^\dagger\mathbf{\Phi}_d\right\rangle-\left\langle\mathbf{\Phi}_d^\dagger\sigma_z\mathbf{T}_{k_\alpha}\mathbf{\Psi}_{k_\alpha}\right\rangle\\&=\sum_k\mathrm{Tr}\left[\mathbf{G}_{d,k_\alpha}^<(t,t)\sigma_z\mathbf{T}_{k_\alpha}(t)\right]+\text{H.c.}.\end{aligned}$$

Here, the nonequilibrium integral $\mathbf{G}_{d,k_\alpha}^<(t,t')$ [17,52] is defined in the 2×2 Nambu representation

$$\mathbf{G}_{d,k_\alpha}^<(t,t')=i\begin{pmatrix}\left\langle c_{k_\alpha\uparrow}^\dagger(t')d_\uparrow(t)\right\rangle & \left\langle c_{-k_\alpha\downarrow}(t')d_\uparrow(t)\right\rangle\\ \left\langle c_{k_\alpha\uparrow}^\dagger(t')d_\downarrow^\dagger(t)\right\rangle & \left\langle c_{-k_\alpha\downarrow}(t')d_\downarrow^\dagger(t)\right\rangle\end{pmatrix},$$

and defined on a two-branch contour that represents the system's evolution from $t=-\infty$ to time t (the upper branch) and then back from time t to $-\infty$. It is necessary to express $\mathbf{G}_{d,k_\alpha}^<(t,t')$, as defined on this contour, in terms of the Green's function of the scattering region $\mathbf{G}$ and the Green's function of the lead $\mathbf{g}_{k_\alpha}$, both of which are defined on the real-time axis. This is achieved by utilizing the Keldysh contour integral technique and the Langreth theorem for analytic continuation.

With the aid of these nonequilibrium Keldysh Green's functions, the current $J_\alpha(t)$ through the αth superconducting lead to the quantum dot is given by [17,50–52,55,56]

$$\begin{aligned}J_\alpha(t)=2\,\mathrm{Re}\int_{-\infty}^t dt'\,\mathrm{Tr}\big\{\big[&\mathbf{G}^r(t,t')\mathbf{\Sigma}_\alpha^<(t',t)\\&+\mathbf{G}^<(t,t')\mathbf{\Sigma}_\alpha^a(t',t)\big]\sigma_z\big\},\end{aligned}\tag{2}$$

where $\mathbf{G}^{r,<}(t,t')$ represent the retarded and lesser Green's functions of the scattering region, respectively, under the influence of a time-dependent voltage. The self-energies $\mathbf{\Sigma}_\alpha^{<,a}(t',t)=\sum_{k_\alpha}\mathbf{T}_{k_\alpha}^\dagger\mathbf{g}_{k_\alpha}^{<,a}\mathbf{T}_{k_\alpha}$ are the lesser and advanced self-energy contributed by the αth superconducting lead with a time-dependent voltage $V_\alpha(t)$. According to the definition of $\mathbf{G}^r(t,t')$ and $\mathbf{\Sigma}^a(t',t)$, we have set the upper limit of the time integration to t. From the tunneling Hamiltonian $\mathbf{T}_{k_\alpha}(t)=\mathbf{T}_{k_\alpha}^0\mathbf{W}_\alpha(t)$, we deduce that

$$\mathbf{\Sigma}_\alpha^\gamma(t',t)=\mathbf{W}_\alpha^\dagger(t')\mathbf{\Sigma}_\alpha^{\gamma,0}(t'-t)\mathbf{W}_\alpha(t),\tag{3}$$

where $\mathbf{\Sigma}_\alpha^{\gamma,0}(t'-t)$ is derived from the superconducting leads with zero voltage. $\mathbf{\Sigma}_\alpha^{\gamma,0}$ is time-difference dependent and can be expressed in the form of a Fourier integral

$$\mathbf{\Sigma}_\alpha^{\gamma,0}(t'-t)=\int\frac{d\epsilon}{2\pi}e^{-i\epsilon(t'-t)}\mathbf{\Sigma}_\alpha^{\gamma,0}(\epsilon).$$

Equation (3) is then expressed as

$$\mathbf{\Sigma}_\alpha^\gamma(t',t)=\int\frac{d\epsilon}{2\pi}e^{-i\epsilon(t'-t)}\mathbf{W}_\alpha^\dagger(t')\mathbf{\Sigma}_\alpha^{\gamma,0}(\epsilon)\mathbf{W}_\alpha(t),$$

where $\gamma=a,<$. For brevity, $\mathbf{\Sigma}_\alpha^{\gamma,0}(\epsilon)$ is detailed in Appendix A. Introducing $\tilde{\mathbf{\Sigma}}_\alpha^\gamma(t',t,\epsilon)=\mathbf{W}_\alpha^\dagger(t')\mathbf{\Sigma}_\alpha^{\gamma,0}(\epsilon)\mathbf{W}_\alpha(t)$, the current $J_\alpha(t)$ in Eq. (2) is expressed as

$$\begin{aligned}J_\alpha(t)=2\,\mathrm{Re}\int\frac{d\epsilon}{2\pi}\int_{-\infty}^t dt'\,e^{i\epsilon(t-t')}\mathrm{Tr}\big[&\mathbf{G}^r(t,t')\tilde{\mathbf{\Sigma}}_\alpha^<(t',t,\epsilon)\sigma_z\\&+\mathbf{G}^<(t,t')\tilde{\mathbf{\Sigma}}_\alpha^a(t',t,\epsilon)\sigma_z\big],\end{aligned}\tag{4}$$

where the first and second terms represent the current flowing into the scattering region $J_\alpha^{\rm in}(t)$ and the current flowing out from the scattering region $J_\alpha^{\rm out}(t)$, respectively [51].

To present physics more effectively, we introduce time-dependent spectral functions, that is defined as [21,22,24,51]

$$\mathbf{A}_\alpha(t,\epsilon)=\int_{-\infty}^t dt'\,e^{i\epsilon(t-t')}\mathbf{G}^r(t,t')\mathbf{W}_\alpha^\dagger(t'),\tag{5}$$

and the incoming current becomes

$$J_\alpha^{\rm in}(t)=2\,\mathrm{Re}\int\frac{d\epsilon}{2\pi}\mathrm{Tr}\big[\mathbf{A}_\alpha(t,\epsilon)\mathbf{\Sigma}_\alpha^{<,0}(\epsilon)\mathbf{W}_\alpha(t)\sigma_z\big].\tag{6}$$

Beyond the wide-band limit, $\mathbf{\Sigma}_\alpha^{r,0}(\epsilon)$ becomes energy dependent, and $\mathbf{G}^r$ becomes a double-time Green's function. To calculate $\mathbf{G}^<$ in Eq. (4), a time integral over a double-time interval is required,

$$\mathbf{G}^<(t,t')=\int dt_1dt_2\sum_\beta\mathbf{G}^r(t,t_1)\mathbf{\Sigma}_\beta^<(t_1,t_2)\mathbf{G}^a(t_2,t').\tag{7}$$

Then, the outgoing current is given by

$$J_\alpha^{\rm out}(t) = 2\,{\rm Re}\sum_\beta \int \frac{d\epsilon}{2\pi}\,{\rm Tr}\big[\mathbf{A}_\beta(t,\epsilon)\mathbf{\Sigma}_\beta^{<,0}(\epsilon) \times \mathbf{Q}_{\beta\alpha}(t,\epsilon)\mathbf{W}_\alpha(t)\sigma_z\big], \tag{8}$$

where $\mathbf{Q}_{\beta\alpha}(t,\epsilon)$ is defined as

$$\mathbf{Q}_{\beta\alpha}(t,\epsilon) = \int \frac{dE}{2\pi} e^{i(E-\epsilon)t}\int_{-\infty}^{t} dt' e^{i(\epsilon-E)t'} \mathbf{A}_\beta^\dagger(t',\epsilon)\mathbf{W}_\alpha^\dagger(t')\mathbf{\Sigma}_\alpha^{a,0}(E). \tag{9}$$

Equations (6) and (8) present our principal theoretical results. Once the retarded Green's function $\mathbf{G}^r(t,t')$ is determined, the spectral function $\mathbf{A}_\alpha(t,\epsilon)$ and the correlation function $\mathbf{Q}_{\beta\alpha}(t,\epsilon)$ can be readily computed. Subsequently, the calculation of the incoming $J_\alpha^{\rm in}(t)$ and outgoing $J_\alpha^{\rm out}(t)$ currents is straightforward. For $t<0$, the current is characterized as a steady phase-biased direct current (dc) for the upwards step-like bias, or as a steady voltage-biased alternating current (ac) for the downwards step-like bias, respectively. These characteristics have been thoroughly researched, with demonstrations provided exclusively in Appendices A and B. Moving forward, our analysis focuses solely on the calculation of the current for $t>0$, which accounts for the transient response following the sudden change in bias.

C. $\mathbf{G}^r(t,t')$ and $\mathbf{A}_\alpha(t,\epsilon)$

We proceed to solve the retarded Green's function $\mathbf{G}^r(t,t')$ using the Dyson equation, focusing on times $t>0$. In our approach, we utilize the "partition-free approach", where the isolated scattering region and superconducting leads are perpetually connected, from $t=-\infty$ to $t=\infty$. The variation induced by the time-dependent bias $\tilde V(t)$ is treated as an interaction that contributes to the Keldysh self-energy. To apply the Dyson equation, we divide the Hamiltonian into two parts: the unperturbed Hamiltonian, which can be exactly solved, and the interaction term due to $\tilde V(t)$. The Green's function of the unperturbed system, symbolically represented as $\bar{\mathbf{G}}^r(t,t')$, represents the system's behavior in its remote future, as $t\to\infty$. It is presumed to be known, with comprehensive details provided in Appendices A and B. The self-energy within the Dyson equations, which we refer to as the time-dependent self-energy, arises from the difference when the interaction term $\tilde V(t)$ is included. This time-dependent self-energy includes two main components. One is derived from the induced internal potential $\mathbf{U}(t)=u_L\tilde V_L(t)\sigma_z$, and the other is due to the change in the left superconducting self-energy when $\tilde V(t)$ is applied, expressed as $\Delta\mathbf{\Sigma}_L^r(t_1,t_2)=\mathbf{\Sigma}_L^r(t_1,t_2)-\bar{\mathbf{\Sigma}}_L^r(t_1,t_2)$. Here, $\bar{\mathbf{\Sigma}}_L^r(t_1,t_2)$ represents the superconducting self-energy of the unperturbed system, i.e., $\tilde V(t)=0$.

Using these time-dependent self-energies, we formulate the Dyson equation in the time domain,

$$\mathbf{G}^r(t,t') = \big\{\bar{\mathbf{G}}^r + [\bar{\mathbf{G}}^r\mathbf{U}\mathbf{G}^r] + \big[\big[\bar{\mathbf{G}}^r\Delta\mathbf{\Sigma}_L^r\mathbf{G}^r\big]\big]\big\}(t,t'). \tag{10}$$

To avoid overly lengthy formulas, we have introduced symbols, which are defined as follows:

$$[\bar{\mathbf{G}}\mathbf{U}\mathbf{G}](t,t') = \int dt_1\,\bar{\mathbf{G}}(t,t_1)\mathbf{U}(t_1)\mathbf{G}(t_1,t'),$$

$$[[\bar{\mathbf{G}}\Delta\mathbf{\Sigma}\mathbf{G}]](t,t') = \int dt_1\int dt_2\,\bar{\mathbf{G}}(t,t_1)\Delta\mathbf{\Sigma}(t_1,t_2)\mathbf{G}(t_2,t').$$

Given that $\tilde V(t>0)=0$, it follows that $\mathbf{U}(t)$ is zero for $t>0$, and $\mathbf{\Sigma}_L^r(t_1,t_2)=\bar{\mathbf{\Sigma}}_L^r(t_1,t_2)$ when $t_1,t_2\in[0,t]$. Consequently, in the Eq. (10), the time integrations are limited to the intervals $\int dt_1=\int_{-\infty}^0 dt_1$ and $\int dt_1\int dt_2=\int_{-\infty}^0 dt_1\int_{-\infty}^{t_1} dt_2+\int_0^t dt_1\int_{-\infty}^0 dt_2$, respectively. Substituting the Eq. (10) into the expression for the spectral function (5), and corresponding to the three terms of $\mathbf{G}^r(t,t')$, we express the spectral function as

$$\mathbf{A}_\alpha(t>0,\epsilon) = \mathbf{A}_{1,\alpha}+\mathbf{A}_{2,\alpha}+\mathbf{A}_{3,\alpha}, \tag{11}$$

where

$$\mathbf{A}_{1,\alpha} = \int_{-\infty}^{t} dt'\,e^{i\epsilon(t-t')}\bar{\mathbf{G}}^r(t,t')\mathbf{W}_\alpha(t'),$$

$$\mathbf{A}_{2,\alpha} = \int_{-\infty}^{0} dt_1\,e^{i\epsilon(t-t_1)}\bar{\mathbf{G}}^r(t,t_1)\mathbf{U}(t_1)\mathbf{A}_\alpha(t_1<0,\epsilon),$$

$$\mathbf{A}_{3,\alpha} = \left(\int_{-\infty}^{0} dt_1\int_{-\infty}^{t_1} dt_2+\int_0^t dt_1\int_{-\infty}^0 dt_2\right) \times e^{i\epsilon(t-t_2)}\bar{\mathbf{G}}^r(t,t_1)\Delta\mathbf{\Sigma}_L^r(t_1,t_2)\mathbf{A}_\alpha(t_2<0,\epsilon).$$

On the right-hand side of the Eq. (11), $\mathbf{A}_\alpha(\epsilon,t<0)$ is determinable, as it is solely contingent upon $\mathbf{G}^r(t<0,t'<0)$, which corresponds to the system's Green's function in its distant past steady states as $t\to-\infty$. It should be noted $\mathbf{G}^r(t<0,t'<0)$ is distinct from unperturbed Green's function $\bar{\mathbf{G}}^r(t,t')$, which describes the system's behavior in its distant future, as $t\to\infty$.

For the downwards case, where $V_L(t)=\tilde V(t)$, we consider the zero-biased nonequilibrium system as the unperturbed system. Accordingly, the internal potential matrix is $\mathbf{U}(t<0)=\mathbf{U}=u_LV\sigma_z$, the unperturbed Green's function is $\bar{\mathbf{G}}^r(t,t_1)=\mathbf{G}^{r,0}(t-t_1)$, and the unperturbed superconducting self-energy is $\bar{\mathbf{\Sigma}}_L^r(t_1,t_2)=\mathbf{\Sigma}_L^{r,0}(t_1-t_2)$. Here, $\mathbf{G}^{r,0}(t-t_1)$ and $\mathbf{\Sigma}_L^{r,0}(t_1-t_2)$ represent the total Green's function and self-energy of the nonequilibrium system under zero bias (see in Appendix A). For the upwards case, $V_L(t)=V-\tilde V(t)$ includes both a steady bias V and a time-dependent bias $\tilde V(t)$. To eliminate future uncertainties, the time-dependent perturbing term should be zero for $t>0$, thus we categorize V into the unperturbed part. This implies that the unperturbed system is the nonequilibrium system with a steady bias V. Consequently, we can express the internal potential matrix as $\mathbf{U}(t<0)=-\mathbf{U}=-u_LV\sigma_z$, the unperturbed Green's function as $\bar{\mathbf{G}}^r(t,t')=\mathbf{G}^{r,V}(t,t')$, and the unperturbed superconducting self-energy as $\bar{\mathbf{\Sigma}}_L^r(t_1,t_2)=\mathbf{\Sigma}_L^{r,V}(t_1,t_2)$ for the upwards case (see in Appendix B). Taking the Fourier transform, the Green's function and self-energy of the unperturbed system with zero bias in the downwards case can be

formulated as

$$\mathbf{G}^{r,0}(t_1-t_2)=\int\frac{d\epsilon}{2\pi}e^{-i\epsilon(t_1-t_2)}\mathbf{G}^{r,0}(\epsilon),$$
$$\mathbf{\Sigma}^{r,0}_{\beta}(t_1-t_2)=\int\frac{d\epsilon}{2\pi}e^{-i\epsilon(t_1-t_2)}\mathbf{\Sigma}^{r,0}_{\beta}(\epsilon).$$

Similarly, for the upwards case with a steady bias V, the Green's function and self-energy of the unperturbed system can be expressed as

$$\mathbf{G}^{r,V}(t_1,t_2)=\int\frac{d\epsilon}{2\pi}\sum_l e^{-il\omega t_1}e^{-i\epsilon(t_1-t_2)}\mathbf{G}^{r,V}_{l0}(\epsilon),$$
$$\mathbf{\Sigma}^{r,V}_{L}(t_1,t_2)=\int\frac{d\epsilon}{2\pi}\sum_l e^{-il\omega t_1}e^{-i\epsilon(t_1-t_2)}\mathbf{\Sigma}^{r,V}_{L,l0}(\epsilon),$$

with $\omega=2V$. Here, $\mathbf{F}_{l0}(\epsilon)=\mathbf{F}(\epsilon+l\omega,\epsilon)$ represents the Fourier coefficient of the double-time Green's function and double-time self-energy for a system with a periodic potential. Additionally, given that $V_R(t)=0$, the self-energy for the right lead is $\mathbf{\Sigma}^{r,0}_R(t_1-t_2)=\int\frac{d\epsilon}{2\pi}e^{-i\epsilon(t_1-t_2)}\mathbf{\Sigma}^{r,0}_R(\epsilon)$. For the sake of brevity, all unperturbed Green's functions $\mathbf{G}^{r,0/V}(\epsilon)$ and self-energies $\mathbf{\Sigma}^{r,0/V}_{\beta}(\epsilon)$ are detailed in the Appendices A and B. Utilizing these unperturbed functions, we can derive $\mathbf{A}_{\alpha}(t,\epsilon)$ and subsequently $\mathbf{Q}_{\beta\alpha}(t,\epsilon)$. In the subsequent sections, we will derive $\mathbf{A}^{D/U}_{\alpha,\sigma\sigma'}(t,\epsilon)$ and $\mathbf{Q}^{D/U}_{\beta\alpha,\sigma\sigma'}(t,\epsilon)$ for the downwards and upwards cases, respectively.

D. $\mathbf{A}^{D/U}_{\beta}(t,\epsilon)$ and $\mathbf{Q}^{D/U}_{\beta\alpha}(t,\epsilon)$

For the sake of conciseness, we introduce the following temporary variables:

$$\vec{\mathbf{A}}^{D}_{\beta,\sigma\sigma'}(t,\epsilon)=\mathbf{A}^{D}_{\beta,\sigma\sigma'}(t,\epsilon-\sigma' V_\beta),$$
$$\vec{\mathbf{Q}}^{D}_{\beta\alpha,\sigma\sigma'}(t,\epsilon)=\mathbf{Q}^{D}_{\beta\alpha,\sigma\sigma'}(t,\epsilon-\sigma V_\beta),$$
$$\vec{\mathbf{\Sigma}}^{a,0}_{\alpha,l,\sigma\sigma'}(\epsilon)=\mathbf{\Sigma}^{a,0}_{\alpha,l,\sigma\sigma'}(\epsilon-\sigma V_\alpha),$$

where $\mathbf{\Sigma}^{a,0}_{l}(\epsilon)=\mathbf{\Sigma}^{a,0}(\epsilon+l\omega)$ and $\sigma,\sigma'=\pm1$ represent the electron and hole matrix elements in Nambu space. As previously analyzed in Sec. II C, when $t<0$, we have $\mathbf{G}^{r}(t,t')=\mathbf{G}^{r,V}(t,t')$ for the downwards case and $\mathbf{G}^{r}(t,t')=\mathbf{G}^{r,0}(t-t')$ for the upwards case. Employing the Fourier transform and the residue theorem, we derive the following expressions from Eqs. (5) and (9):

$$\vec{\mathbf{A}}^{D}_{\beta}(t<0)=\sum_l e^{-il\omega t}\mathbf{G}^{r,V}_{l0}(\epsilon)\bar{\mathbf{W}}^{\dagger}_{\beta}(t),$$
$$\vec{\mathbf{Q}}^{D}_{\beta\alpha}(t<0)=\sum_l e^{il\omega t}\bar{\mathbf{W}}_{\beta}(t)\mathbf{G}^{a,V}_{0l}(\epsilon)\bar{\mathbf{W}}^{\dagger}_{\alpha}(t)\vec{\mathbf{\Sigma}}^{a,0}_{\alpha,l}(\epsilon),$$
$$\mathbf{A}^{U}_{\beta}(t<0)=\mathbf{G}^{r,0}(\epsilon),$$
$$\mathbf{Q}^{U}_{\beta\alpha}(t<0)=\mathbf{G}^{a,0}(\epsilon)\mathbf{\Sigma}^{a,0}_{\alpha}(\epsilon). \tag{12}$$

It should be noted that the current is the result of an infinite integral over ϵ of $\mathbf{A}_{\beta}(\epsilon)$ and $\mathbf{Q}_{\beta\alpha}(\epsilon)$, thus permitting the energy shift $\epsilon+\sigma V_\beta$.

Moving forward, we focus on $\mathbf{A}_{\beta}(t>0,\epsilon)$ and $\mathbf{Q}_{\beta\alpha}(t>0,\epsilon)$. Substituting Eq. (10) into Eq. (11) and applying the residue theorem, we obtain the spectral function for the downwards case as follows:

$$\vec{\mathbf{A}}^{D}_{\beta}(t>0)=\left[\vec{\mathbf{A}}^{D}_{1}+\sum_l\left(\vec{\mathbf{A}}^{D}_{2}+\vec{\mathbf{A}}^{D}_{3}\right)\right]\bar{\mathbf{W}}^{\dagger}_{\beta}(t), \tag{13}$$

with

$$\vec{\mathbf{A}}^{D}_{1}=\vec{\mathbf{G}}^{r,0}_{\beta}(\epsilon)\bar{\mathbf{W}}_{\beta}(t)+\|\mathbf{G}^{r,0}(\mathbf{Z}_0-\mathbf{Z}_{1_\beta})\|,$$
$$\vec{\mathbf{A}}^{D}_{2}=\|\mathbf{G}^{r,0}\mathbf{U}\mathbf{Z}_{0,l}\|\mathbf{G}^{r,V}_{l0}(\epsilon),$$
$$\vec{\mathbf{A}}^{D}_{3}=\Big\|\mathbf{G}^{r,0}\Big\{\Big[\mathbf{\Sigma}^{r,0}_{L}(E)-\vec{\mathbf{\Sigma}}^{r,0}_{L,l}(\epsilon)\Big]\mathbf{Z}_{1_V,l}+\Big[\vec{\mathbf{\Sigma}}^{r,0}_{L,l}(\epsilon)\cdot\mathbf{Z}_{2_V,l}-\mathbf{\Sigma}^{r,0}_{L}(E)\mathbf{Z}_{0,l}\Big]\Big\}\Big\|\mathbf{G}^{r,V}_{l0}(\epsilon).$$

Here, '$\cdot$' denotes the matrix element multiplication. For brevity, we introduce additional temporary variables,

$$\vec{\mathbf{G}}^{r,0}_{\beta,\sigma\sigma'}(\epsilon)=\mathbf{G}^{r,0}_{\sigma\sigma'}(\epsilon-\sigma' V_\beta),$$
$$\vec{\mathbf{G}}^{a,0}_{\beta,\sigma\sigma'}(\epsilon)=\mathbf{G}^{a,0}_{\sigma\sigma'}(\epsilon-\sigma V_\beta,),$$
$$\vec{\mathbf{\Sigma}}^{r,0}_{L,\sigma\sigma'}(\epsilon)=\mathbf{\Sigma}^{r,0}_{L,\sigma\sigma'}(\epsilon-\sigma' V),$$
$$\vec{\mathbf{\Sigma}}^{a,0}_{L,\sigma\sigma'}(\epsilon)=\mathbf{\Sigma}^{a,0}_{L,\sigma\sigma'}(\epsilon-\sigma V),$$

notations for the integral,

$$\|\mathbf{GF}\|(t,\epsilon)=\int\frac{dE}{2\pi}e^{i(\epsilon-E)t}\mathbf{G}(E)\mathbf{F}(E,\epsilon),$$

and the abbreviation of N-dimensional array in Nambu space $\mathbf{Z}_N$, which is defined as follows:

$$\mathbf{Z}_{N,l}=\mathbf{Z}_N(E,\epsilon+l\omega),$$
$$\mathbf{Z}_0(E,\epsilon)=-i(E-\epsilon-i0_+)^{-1},$$
$$\mathbf{Z}_{1_\beta}(E,\epsilon)=-i(E-\epsilon+\sigma_z V_\beta-i0_+)^{-1},$$
$$\mathbf{Z}_{1_V}(E,\epsilon)=-i(E-\epsilon+\sigma_z V-i0_+)^{-1},$$
$$\mathbf{Z}_{2_V,\sigma\sigma'}(E,\epsilon)=-i(E-\epsilon-(\sigma-\sigma')V-i0_+)^{-1},$$

where σ_z is Pauli matrix. In Eq. (13), we have left out the dummy index σ_i that just indicates summation in the matrix multiplication. Finally, from Eqs. (13) and (9), we can express $\vec{\mathbf{Q}}^{D}_{\beta\alpha}(t>0,\epsilon)$ as

$$\vec{\mathbf{Q}}^{D}_{\beta\alpha}(t>0,\epsilon)=\bar{\mathbf{W}}_{\beta}(t)\left[\vec{\mathbf{Q}}^{D}_{0}+\vec{\mathbf{Q}}^{D}_{1}+\sum_l\left(\vec{\mathbf{Q}}^{D}_{2}+\vec{\mathbf{Q}}^{D}_{3}\right)\right], \tag{14}$$

with

$$\vec{\mathbf{Q}}^{D}_{0}=\sum_l\Big\|\mathbf{G}^{a,V}_{0l}(\epsilon)\mathbf{Z}^{\dagger}_{1_\alpha,l}\mathbf{\Sigma}^{a,0}\Big\|-\Big\|\mathbf{Z}^{\dagger}_{1_\beta}\vec{\mathbf{G}}^{a,0}_{\beta}(\epsilon)\mathbf{\Sigma}^{a,0}\Big\|,$$
$$\vec{\mathbf{Q}}^{D}_{1}=\bar{\mathbf{W}}^{\dagger}_{\beta}(t)\left\lceil\vec{\mathbf{G}}^{a,0}\mathbf{\Sigma}^{a,0}_{\alpha}\right\rceil_{\beta}+\Big\|\left(\mathbf{Z}^{\dagger}_{0}-\mathbf{Z}^{\dagger}_{1_\beta}\right)\mathbf{G}^{a,0}\left\lfloor\mathbf{\Sigma}^{a,0}_{\alpha}\right\rfloor\Big\|,$$
$$\vec{\mathbf{Q}}^{D}_{2}=\mathbf{G}^{a,V}_{0l}(\epsilon)\Big\|\mathbf{Z}^{\dagger}_{0,l}\mathbf{U}\mathbf{G}^{a,0}\left\lfloor\mathbf{\Sigma}^{a,0}_{\alpha}\right\rfloor\Big\|,$$
$$\vec{\mathbf{Q}}^{D}_{3}=\mathbf{G}^{a,V}_{0l}(\epsilon)\Big\|\Big\{\mathbf{Z}^{\dagger}_{1_V,l}\Big[\mathbf{\Sigma}^{a,0}_{L}(E)-\vec{\mathbf{\Sigma}}^{a,0}_{L,l}(\epsilon)\Big]+\Big[\vec{\mathbf{\Sigma}}^{a,0}_{L,l}(\epsilon)\cdot\mathbf{Z}^{\dagger}_{2_V,l}-\mathbf{\Sigma}^{a,0}_{L}(E)\mathbf{Z}^{\dagger}_{0,l}\Big]\Big\}\mathbf{G}^{a,0}\left\lfloor\mathbf{\Sigma}^{a,0}_{\alpha}\right\rfloor\Big\|,$$

where

$$\left\lceil\vec{\mathbf{G}}^{a,0}\mathbf{\Sigma}^{a,0}_{\alpha}\right\rceil_{\beta,\sigma\sigma'}=\sum_{\sigma_1}\mathbf{G}^{a,0}_{\sigma\sigma_1}(\epsilon-\sigma V_\beta)\mathbf{\Sigma}^{a,0}_{\alpha,\sigma_1\sigma'}(\epsilon-\sigma V_\beta),$$

and integral abbreviation,

$$\|\mathbf{F}\boldsymbol{\Sigma}\|(t,\epsilon) = \int \frac{dE}{2\pi} e^{-i(\epsilon-E)t}\mathbf{F}(E,\epsilon)\boldsymbol{\Sigma}(E),$$
$$\|\mathbf{F}\mathbf{G}\lfloor\boldsymbol{\Sigma}\rfloor\|(t,\epsilon) = \int \frac{dE}{2\pi} e^{-i(\epsilon-E)t}\mathbf{F}(E,\epsilon)\mathbf{G}(E)\lfloor\boldsymbol{\Sigma}\rfloor(t,E),$$
$$\lfloor\boldsymbol{\Sigma}^{a,0}_{\alpha}\rfloor(t,E) = \int \frac{d\epsilon'}{2\pi}(1-e^{i(\epsilon'-E)t})\mathbf{Z}^{\dagger}_{0}(\epsilon',E)\boldsymbol{\Sigma}^{a,0}_{\alpha}(\epsilon').$$

For the upwards case, we introduce new temporary variables,

$$\vec{\mathbf{G}}^{r,V}_{\beta,l0,\sigma\sigma'}(\epsilon) = \mathbf{G}^{r,V}_{l0,\sigma\sigma'}(\epsilon+\sigma' V_\beta),$$
$$\vec{\mathbf{G}}^{a,V}_{\beta,0l,\sigma\sigma'}(\epsilon) = \mathbf{G}^{a,V}_{0l,\sigma\sigma'}(\epsilon+\sigma V_\beta),$$
$$\vec{\boldsymbol{\Sigma}}^{r,0}_{L,\sigma\sigma'}(E) = \boldsymbol{\Sigma}^{r,0}_{L,\sigma\sigma'}(E-\sigma V),$$
$$\vec{\boldsymbol{\Sigma}}^{a,0}_{L,\sigma\sigma'}(E) = \boldsymbol{\Sigma}^{a,0}_{L,\sigma\sigma'}(E-\sigma' V),$$

and

$$\mathbf{Z}_{1_\alpha}(\epsilon',E) = -i(\epsilon'-E+\sigma_z V_\alpha - i0_+)^{-1},$$
$$\mathbf{Z}_{1_\beta}(E,\epsilon) = -i(E-\epsilon-\sigma_z V_\beta - i0_+)^{-1},$$
$$\mathbf{Z}_{1_V}(E,\epsilon) = -i(E-\epsilon-\sigma_z V - i0_+)^{-1},$$
$$\mathbf{Z}_{2_{\beta\alpha},\sigma\sigma'}(E,\epsilon) = -i(E-\epsilon-\sigma V_\beta+\sigma' V_\alpha - i0_+)^{-1}.$$

Then the spectral function for upwards case is written as

$$\mathbf{A}^{U}_{\beta}(t>0,\epsilon) = \sum_{l} e^{-il\omega t}\left(\mathbf{A}^{U}_{1}+\mathbf{A}^{U}_{2}+\mathbf{A}^{U}_{3}\right), \tag{15}$$

with

$$\mathbf{A}^{U}_{1} = \vec{\mathbf{G}}^{r,V}_{\beta,l0}(\epsilon)\bar{\mathbf{W}}^{\dagger}_{\beta}(t) + \left\|\mathbf{G}^{r,V}_{l0}\left(\mathbf{Z}_0-\mathbf{Z}_{1_\beta}\right)\right\|,$$
$$\mathbf{A}^{U}_{2} = -\left\|\mathbf{G}^{r,V}_{l0}\mathbf{U}\mathbf{Z}_0\right\|\mathbf{G}^{r,0}(\epsilon),$$
$$\mathbf{A}^{U}_{3} = \left\|\mathbf{G}^{r,V}_{l0}\left\{\mathbf{Z}_{1_V}\left[\vec{\boldsymbol{\Sigma}}^{r,0}_{L}(E)-\boldsymbol{\Sigma}^{r,0}_{L}(\epsilon)\right]\right.\right.$$
$$\left.\left.+\left[\mathbf{Z}_0\boldsymbol{\Sigma}^{r,0}_{L}(\epsilon)-\mathbf{Z}_{2_V}\cdot\vec{\boldsymbol{\Sigma}}^{r,0}_{L}(E)\right]\right\}\right\|\mathbf{G}^{r,0}(\epsilon).$$

From Eq. (15) and (9), we can write

$$\mathbf{Q}^{U}_{\beta\alpha}(t>0,\epsilon) = \mathbf{Q}^{U}_{0} + \sum_{l} e^{il\omega t}\left(\mathbf{Q}^{U}_{1}+\mathbf{Q}^{U}_{2}+\mathbf{Q}^{U}_{3}\right), \tag{16}$$

with

$$\mathbf{Q}^{U}_{0} = \|\mathbf{G}^{a,0}(\epsilon)\mathbf{Z}^{\dagger}_{0}\boldsymbol{\Sigma}^{a,0}\| - \sum_{l}\left\|\mathbf{Z}^{\dagger}_{2_{\beta\alpha}}\cdot\vec{\mathbf{G}}^{a,V}_{\beta,0l}(\epsilon)\boldsymbol{\Sigma}^{a,0}\right\|,$$
$$\mathbf{Q}^{U}_{1} = \bar{\mathbf{W}}_{\beta}\left[\vec{\mathbf{G}}^{a,V}_{0l}\bar{\mathbf{W}}^{\dagger}_{\alpha}\vec{\boldsymbol{\Sigma}}^{a,0}_{\alpha,l}\right]_{\beta,\sigma\sigma'} + \left\|(\mathbf{Z}^{\dagger}_{0}-\mathbf{Z}^{\dagger}_{1_\beta})\mathbf{G}^{a,V}_{0l}\lfloor\boldsymbol{\Sigma}^{a,0}_{\alpha}\rfloor\right\|,$$
$$\mathbf{Q}^{U}_{2} = -\mathbf{G}^{a,0}(\epsilon)\left\|\mathbf{Z}^{\dagger}_{0}\mathbf{U}\mathbf{G}^{a,V}_{0l}\lfloor\boldsymbol{\Sigma}^{a,0}_{\alpha}\rfloor\right\|,$$
$$\mathbf{Q}^{U}_{3} = \mathbf{G}^{a,0}(\epsilon)\left\|\left\{\left[\vec{\boldsymbol{\Sigma}}^{a,0}_{L}(E)-\boldsymbol{\Sigma}^{a,0}_{L}(\epsilon)\right]\mathbf{Z}^{\dagger}_{1_V}\right.\right.$$
$$\left.\left.+\left[\mathbf{Z}^{\dagger}_{0}\boldsymbol{\Sigma}^{a,0}_{L}(\epsilon)-\mathbf{Z}^{\dagger}_{2_V}\cdot\vec{\boldsymbol{\Sigma}}^{a,0}_{L}(E)\right]\right\}\mathbf{G}^{a,V}_{0l}\lfloor\boldsymbol{\Sigma}^{a,0}_{\alpha}\rfloor\right\|,$$

where

$$\left[\vec{\mathbf{G}}^{a,V}_{0l}\bar{\mathbf{W}}^{\dagger}_{\alpha}(t)\vec{\boldsymbol{\Sigma}}^{a,0}_{\alpha,l}\right]_{\beta,\sigma\sigma'} = \sum_{\sigma_1}\mathbf{G}^{a,V}_{\beta,0l,\sigma\sigma_1}(\epsilon+\sigma V_\beta)\bar{\mathbf{W}}^{\dagger}_{\alpha,\sigma_1}(t)$$
$$\times\ \boldsymbol{\Sigma}^{a,0}_{\alpha,l,\sigma_1\sigma'}(\epsilon+\sigma V_\beta-\sigma_1 V_\alpha),$$

and the integral abbreviation,

$$\|\mathbf{F}\boldsymbol{\Sigma}\|(t,\epsilon) = \int \frac{dE}{2\pi} e^{-i(\epsilon-E)t}\mathbf{F}(E,\epsilon)\boldsymbol{\Sigma}(E),$$
$$\|\mathbf{F}\mathbf{G}\lfloor\boldsymbol{\Sigma}\rfloor\|(t,\epsilon) = \int \frac{dE}{2\pi} e^{-i(\epsilon-E)t}\mathbf{F}(E,\epsilon)\mathbf{G}(E)\lfloor\boldsymbol{\Sigma}\rfloor(t,E),$$
$$\lfloor\boldsymbol{\Sigma}^{a,0}_{\alpha}\rfloor = \int \frac{d\epsilon'}{2\pi}[\bar{\mathbf{W}}^{\dagger}_{\alpha}(t) - e^{i(\epsilon'-E-l\omega)t}]\mathbf{Z}^{\dagger}_{1_\alpha,l}(\epsilon',E)$$
$$\times\ \boldsymbol{\Sigma}^{a,0}_{\alpha}(\epsilon').$$

E. The limits of $t = 0$ and $t \to \infty$

We examine two limits: the initial current at $t = 0$ and the asymptotic current as $t \to \infty$. Physically, the asymptotic current $J^{D/U}(t\to\infty)$ for the downwards (upwards) case is equivalent to the initial current $J^{U/D}(t<0)$ for the upwards (downwards) case. Mathematically, these initial and asymptotic currents can be directly computed from the standard phase/voltage-biased nonequilibrium Green's function, namely the unperturbed Green's function $\mathbf{G}^{r,0/V}$, as depicted in Eq. (12). We will now demonstrate that the limits of the general expression, Eqs. (13)–(16), are consistent with unperturbed results. At the moment of $t = 0$, the term $e^{i(\epsilon-E)t}$ does not diverge in the upper half-plane of E. This allows us to execute the integration over energy E in Eqs. (13) and (15) by enclosing a contour in the upper half-plane, where a single residue is present at the energy pole of $\mathbf{Z}_N$. Consequently, we obtain the following results:

$$\begin{aligned}\vec{\mathbf{A}}^{D}_{\beta}(t=0) &= \mathbf{G}^{r,0} + \sum_{l}\left[\mathbf{G}^{r,0}U\mathbf{G}^{r,V}\right.\\ &\quad\left.+\mathbf{G}^{r,0}\left(\boldsymbol{\Sigma}^{r,V}_{L}-\boldsymbol{\Sigma}^{r,0}_{L}\right)\mathbf{G}^{r,V}\right]_{l0}\\ &= \sum_{l}\mathbf{G}^{r,V}_{l0}(\epsilon),\\ \mathbf{A}^{U}_{\beta}(t=0) &= \sum_{l}\left[\mathbf{G}^{r,V}-\mathbf{G}^{r,V}U\mathbf{G}^{r,0}\right.\\ &\quad\left.-\mathbf{G}^{r,V}\left(\boldsymbol{\Sigma}^{r,V}_{L}-\boldsymbol{\Sigma}^{r,0}_{L}\right)\mathbf{G}^{r,0}\right]_{l0}\\ &= \mathbf{G}^{r,0}(\epsilon).\end{aligned} \tag{17}$$

For the expression of $\mathbf{Q}_{\beta\alpha}$, $\lfloor\boldsymbol{\Sigma}^{a,0}_{\alpha}\rfloor = 0$, the second term of $\mathbf{Q}_0$ and the first term of $\mathbf{Q}_1$ cancel out with each other. Similar to $\vec{\mathbf{A}}^{D}_{\beta}(t=0)$ and $\mathbf{A}^{U}_{\beta}(t=0)$, $\mathbf{Q}_{\beta\alpha}$ simplifies to

$$\vec{\mathbf{Q}}^{D}_{\beta\alpha}(t=0) = \sum_{l}\mathbf{G}^{a,V}_{0l}(\epsilon)\vec{\boldsymbol{\Sigma}}^{a,0}_{\alpha,l}(\epsilon),$$
$$\mathbf{Q}^{U}_{\beta\alpha}(t=0) = \mathbf{G}^{a,0}(\epsilon)\boldsymbol{\Sigma}^{a,0}_{\alpha}(\epsilon). \tag{18}$$

It is found that Eqs. (17) and (18) are identical to the expressions (12) with t fixed at zero, that is derived from the unperturbed Green's function.

As $t \to \infty$, invoking the Riemann-Lebesgue lemma [57], the Fourier integral over E tends to zero. This is because there are always poles located in the lower half of the complex plane, which leads to the integral $\int \frac{dE}{2\pi}e^{-iEt}\mathbf{G}^{r}(E)\ldots$ vanishing as t approaches infinity. With this consideration, the

asymptotic expressions for the spectral functions become

$$\mathbf{A}^D_\beta(t\to\infty)=\mathbf{G}^{r,0}(\epsilon),$$
$$\vec{\mathbf{A}}^U_\beta(t\to\infty)=\sum_l e^{-il\omega t}\mathbf{G}^{r,V}_{l0}(\epsilon)\bar{\mathbf{W}}^\dagger_\beta(t). \tag{19}$$

According to the Riemann-Lebesgue lemma, the Fourier integrals $\int\frac{dE}{2\pi}e^{iEt}\mathbf{\Sigma}^a(E)\ldots$ or $\int\frac{dE}{2\pi}e^{iEt}\mathbf{G}^a(E)\ldots$ also vanish. Consequently, $\mathbf{Q}_0$, the second term of $\mathbf{Q}_1$, $\mathbf{Q}_2$, and $\mathbf{Q}_3$ are all equal to zero. Thus, the $\mathbf{Q}_{\beta\alpha}$ terms simplify to

$$\mathbf{Q}^D_{\beta\alpha}(t\to\infty)=\mathbf{G}^{a,0}(\epsilon)\mathbf{\Sigma}^{a,0}_\alpha(\epsilon),$$
$$\vec{\mathbf{Q}}^U_{\beta\alpha}(t\to\infty)=\sum_l e^{il\omega t}\bar{\mathbf{W}}_\beta(t)\mathbf{G}^{a,V}_{0l}(\epsilon)\bar{\mathbf{W}}^\dagger_\alpha(t)\vec{\mathbf{\Sigma}}^{a,0}_{\alpha,l}(\epsilon). \tag{20}$$

Comparing these results with Eq. (12), it is evident that $\mathbf{A}^{D/U}(t\to\infty)=\mathbf{A}^{U/D}(t<0)$ and $\mathbf{Q}^{D/U}(t\to\infty)=\mathbf{Q}^{U/D}(t<0)$. This implies that the asymptotic current $J^{D/U}(t\to\infty)$ for the downwards (upwards) case is equivalent to the initial current $J^{U/D}(t<0)$ for the upwards (downwards) case.

From the current Eqs. (6) and (8), and the lesser Green's function (7), we deduce the asymptotic current driven by a downwards step-like bias, expressed as

$$J^D_{\alpha,\text{in}}(t\to\infty)=\int\frac{d\epsilon}{2\pi}\mathbf{G}^{r,0}(\epsilon)\mathbf{\Sigma}^{<,0}_\alpha(\epsilon),$$
$$J^D_{\alpha,\text{out}}(t\to\infty)=\int\frac{d\epsilon}{2\pi}\mathbf{G}^{<,0}(\epsilon)\mathbf{\Sigma}^{a,0}_\alpha(\epsilon), \tag{21}$$

where

$$\mathbf{G}^{<,0}(\epsilon)=\sum_\beta\mathbf{G}^{r,0}(\epsilon)\mathbf{\Sigma}^{<,0}_\beta(\epsilon)\mathbf{G}^{a,0}(\epsilon).$$

Utilizing the expressions of the biased unperturbed Green's function (B1) and self-energy (B2) and (B3), we obtain the asymptotic current for the upwards case

$$J^U_{\alpha,\text{in}}(t\to\infty)=\sum_{l\delta}e^{-i(l-\delta)\omega t}\int\frac{d\epsilon}{2\pi}\mathbf{G}^{r,V}_{l0}(\epsilon)\mathbf{\Sigma}^{<,V}_{\alpha,0\delta}(\epsilon),$$
$$J^U_{\alpha,\text{out}}(t\to\infty)=\sum_{ll'\delta\delta',\beta}e^{-i(l-l'-\delta-\delta')\omega t}\int\frac{d\epsilon}{2\pi}\times\mathbf{G}^{r,V}_{l0}\mathbf{\Sigma}^{<,V}_{\beta,0\delta}\mathbf{G}^{a,V}_{\delta,l'+\delta}\mathbf{\Sigma}^{a,V}_{\alpha,l'+\delta,l'+\delta+\delta'}. \tag{22}$$

Here, the integration variable ϵ and the summation targets l, l' can be optionally shifted, allowing Eq. (22) to be rewritten as

$$J^U_{\alpha,\text{in}}(t\to\infty)=\sum_{l\delta}e^{i(l+\delta)\omega t}\int\frac{d\epsilon}{2\pi}\mathbf{G}^{r,V}_{0l}(\epsilon)\mathbf{\Sigma}^{<,V}_{\alpha,l,l+\delta}(\epsilon),$$
$$J^U_{\alpha,\text{out}}(t\to\infty)=\sum_{l\delta}e^{i(l+\delta)\omega t}\int\frac{d\epsilon}{2\pi}\mathbf{G}^{<,V}_{0l}(\epsilon)\mathbf{\Sigma}^{a,V}_{\alpha,l,l+\delta}(\epsilon), \tag{23}$$

with

$$\mathbf{G}^{<,V}_{0l}(\epsilon)=\sum_{l',\delta',\beta}\mathbf{G}^{r,V}_{0l'}(\epsilon)\mathbf{\Sigma}^{<,V}_{\beta,l',l'+\delta'}(\epsilon)\mathbf{G}^{a,V}_{l'+\delta',l}(\epsilon).$$

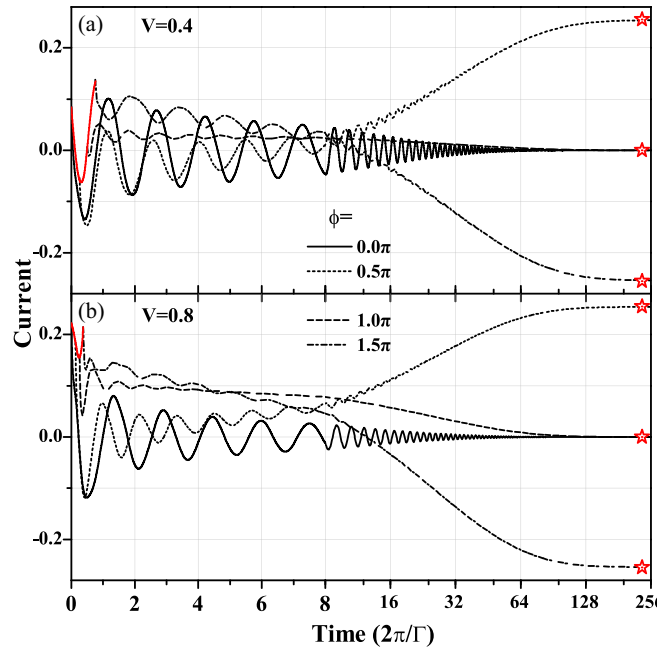

FIG. 3. Time dependence of transient current $J^D(t)$ driven by different downwards step-like biases $V=0.4$ (a) and $V=0.8$ (b). Different lines correspond to different superconducting phase differences ϕ. The other parameter: $\Gamma=0.8$. The initial time $t=0$ is shifted by $\delta t=\phi/\omega$ to show the current oscillation. The initial current with different ϕ forms the ac current before bias is closed, as shown by red lines.

Here, $\mathbf{\Sigma}^{\gamma,V}_{\beta,l,l+\delta}(\epsilon)=\mathbf{\Sigma}^{\gamma,V}_{\beta,0\delta}(\epsilon+l\omega)$ with $\gamma=a,<$ and $\omega=2V$. $\delta=0$ for the diagonal elements $\mathbf{\Sigma}^{\gamma,V}_{\beta,\uparrow\uparrow}$ and $\mathbf{\Sigma}^{\gamma,V}_{\beta,\downarrow\downarrow}$ of the Nambu matrix, and $\delta=\pm1$ for the nondiagonal elements $\mathbf{\Sigma}^{\gamma,V}_{\beta,\downarrow\uparrow}$ and $\mathbf{\Sigma}^{\gamma,V}_{\beta,\uparrow\downarrow}$. The double energy self-energy $\mathbf{\Sigma}^{\gamma,V}_{\beta,\sigma\sigma',0\delta}(\epsilon)=\mathbf{\Sigma}^{\gamma,0}_{\beta,\sigma\sigma'}[\epsilon+\delta\omega_\beta-\sigma' V_\beta]$ with $\omega_\beta=2V_\beta$ is another expression of Eq. (B2), where $\sigma,\sigma'=\pm1$ denotes the electron spin in the Nambu representation.

Now, it is evident that Eqs. (21) and (23) are precisely the dc current expressions in the case of zero bias and the ac current expressions in the case of nonzero bias, respectively.

III. NUMERICAL RESULTS AND DISCUSSIONS

In our numerical calculations, we set the quantum dot energy level $\epsilon_d=0$, $\Gamma_L=\Gamma_R=\Gamma$, ensuring both simplicity and physical plausibility. The superconducting gap $\tilde{\Delta}_L=\tilde{\Delta}_R e^{i\phi}$ Here, $\phi=\phi_L-\phi_R$ signifies the phase difference between the two leads. $\Delta_L=\Delta_R=\Delta=1$ is set as the energy unit.

A. Turning-off transient current

We begin our analysis with the quench dynamics associated with the turning-off process. In Figs. 3(a) and 3(b), we illustrate the transient current J^D induced by a downwards step-like bias with strengths $V=0.4$ and 0.8, respectively. This transient process serves as a transition between the initial ac current, which is present with a finite bias V, and the final dc current when the bias is zero. When the electrons

are injected within the superconducting gap, the supercurrent is determined by the superconducting phase difference ϕ. For the initial ac current, the bias V not only modifies the energy of the Cooper pairs but also impacts the phase of the complex superconducting order parameter $\tilde{\Delta}_\alpha$. Under the influence of V, the phase difference ϕ becomes periodically time dependent, expressed as $\tilde{\phi} = \phi + 2Vt$, wherein ϕ can be considered the initial phase of the alternating current. To clearly demonstrate the alternating current, the beginning time is adjusted by $\delta t = \phi/\omega$. Consequently, the current at the adjusted beginning time for various ϕ values establishes the initial ac current driven by the dc bias V, as depicted by the red lines in Fig. 3. Over the range from $\phi = 0$ to 1.5π, we display three-quarters of a cycle.

Upon examination, the initial current, indicated by the red line in Fig. 3(b), is found to be identical to the steady ac current shown in Fig. 2(c). After a long relaxation period, the transient current ultimately reaches its final dc state. For ease of comparison, we have marked the red stars in Fig. 2(d). A comparison between Fig. 3(b) and Fig. 2(d) reveals that the asymptotic current, derived from the general expression of the transient current, matches the steady theoretical dc current. After the bias is turned off, electrons are unable to tunnel out of the Josephson junction through MARs. Instead, they are trapped within the quantum dot and oscillate between ABSs. This behavior results in the transient current oscillating nearly indefinitely. Due to the presence of these bound states, the relaxation time of the turning-off transient process is considerably lengthy. In addition to the initial and asymptotic currents, the transient current in Fig. 3 exhibits the following characteristics: (1) The transient current oscillates with time, with the oscillation frequency ν varying for different superconducting phases ϕ. From $\phi = 0$ to $\phi = \pi$, ν decreases monotonically. (2) The oscillation frequency ν is nearly identical for $\phi = 0.5\pi$ and $\phi = 1.5\pi$. (3) Upon comparing Figs. 3(a) and 3(b), it is evident that the oscillation frequency ν is independent of the bias V, yet the amplitude of the oscillation is influenced by the bias V. (4) The transient current oscillates nearly indefinitely, with a relaxation time τ that far exceeds $200 \times 2\pi/\Gamma$, which is significantly longer than that observed in conventional quantum transport. It should be noted that to illustrate the extended relaxation time, an exponential time scale is employed for $t > 8 \times 2\pi/\Gamma$.

To understand how the oscillation frequency is affected by the superconducting phase ϕ, we present a plot of ABSs versus ϕ for various coupling strengths Γ in Fig. 4. The energy levels of the ABSs are obtained analytically from the singular points of the Green's function $\mathbf{G}^{r/a,0}$ (see Appendix A). Within the gap region, there exist a pair of bound states with energies $\pm\epsilon_b$. Electrons within the quantum dot oscillate between these two bound states, and the oscillation frequency of the current in Fig. 3 is solely determined by the energy level difference $\Delta\epsilon_b$, irrespective of the external bias V. From Fig. 4, it can be observed that as the coupling strength Γ increases, the energy level ϵ_b gradually approaches the edge of the superconducting gap, i.e., $\epsilon_b \to \pm\Delta$. In the calculations for Fig. 3, $\Gamma = 0.8$ is selected (represented by the dash-dotted lines in Fig. 4). Over the range from $\phi = 0$ to $\phi = 2\pi$, $\pm\epsilon_b$ monotonically decreases (increases) through zero. At $\phi = \pi$, $\pm\epsilon_b = 0$, and there is minimal oscillation when $\phi = \pi$. The

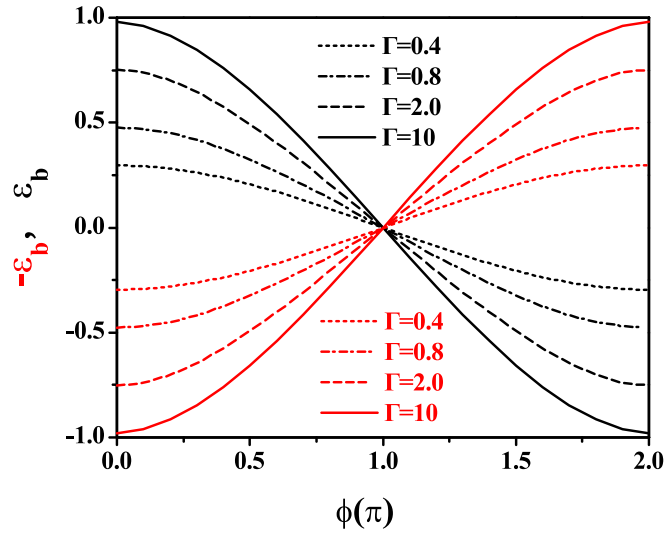

FIG. 4. Andreev bound states energies ϵ_b vs superconducting phase difference ϕ for different Γ.

level spacing between the bound states $\Delta\epsilon_b$ decreases as ϕ changes from 0 to π, exhibiting symmetry with respect to $\phi = \pi$. Consequently, the oscillation frequency decreases from $\phi = 0$ to $\phi = \pi$ and is nearly equivalent for ϕ and $2\pi - \phi$, as depicted in Fig. 3. From the Fig. 3, we can speculate once the bias is turned off, electrons cannot be scattered out of the quantum dot through conventional quantum tunneling; they can only remain within the quantum dot and oscillate between the two bound states within the superconducting gap, as shown in Fig. 1(b). Theoretically, the transient current would continue to oscillate indefinitely and never reach a final state, given the infinite lifetime of the bound states. However, in our calculations, we have introduced an infinitesimally small imaginary part into the incoming energy to prevent calculation divergence. This results in an extremely long, rather than infinite relaxation time.

B. Quasiparticle trapping in turning-off quench dynamics

As discussed in the preceding section, the infinite relaxation time is attributed to the ABSs. During these prolonged relaxation processes, the "turning-off" operation introduces a new periodic oscillation, as depicted in Fig. 3. The oscillation period is determined by the bound states ϵ_b, which is distinct from the ac current oscillation driven by a dc bias. This implies that the bound states ϵ_b influence the exponential oscillation components. In the absence of $\mathbf{G}^{r/a,V}$ with a finite bias, electrons cannot be scattered out of the Josephson junction through multiple Andreev reflections (MARs). Instead, they are trapped. We can identify characteristic terms $\tilde{\mathbf{A}}^D_\beta$ and $\tilde{\mathbf{Q}}^D_{\beta\alpha}$ that include only $\mathbf{G}^{r/a,0}$ and lack $\mathbf{G}^{r/a,V}$. From Eqs. (13) and (14), we derive

$$\tilde{\mathbf{A}}^D_{\beta,\sigma\sigma'}(t,\epsilon) = \mathbf{G}^{r,0}_{\sigma\sigma'}(\epsilon) + \int \frac{dE}{2\pi} \frac{e^{i(\epsilon-E)t}\mathbf{G}^{r,0}_{\sigma\sigma'}(E)}{i(E-\epsilon-\sigma' V_\beta - i0^+)},$$

$$\tilde{\mathbf{Q}}^D_{\beta\alpha,\sigma'\sigma}(t,\epsilon) = \left[\mathbf{G}^{a,0}(\epsilon)\Sigma^{a,0}_\alpha(\epsilon)\right]_{\sigma'\sigma} + \int \frac{dE}{2\pi} \frac{e^{-i(\epsilon-E)t}\left[\mathbf{G}^{a,0}(E)\mathbf{\Sigma}^{a,0}_\alpha(E)\right]_{\sigma'\sigma}}{-i(E-\epsilon-\sigma' V_\beta + i0^+)}.$$

By combining the expression for $\mathbf{G}^{r/a,0}$ Eq. (A1) and applying the residue theorem, we can solve the integral in the aforementioned equation. Subsequently, we obtain

$$\tilde{\mathbf{A}}^{D}_{\beta,\sigma\sigma'} = \mathbf{G}^{r,0}_{\sigma\sigma'}(\epsilon) + \sum_{\pm} \frac{e^{i(\epsilon\mp\epsilon_b)t}\mathbf{P}^{*,r}_{\sigma\sigma'}(\pm\epsilon_b)}{\mp 2\epsilon_b(\pm\epsilon_b - \epsilon - \sigma' V_\beta - i0^+)},$$

$$\tilde{\mathbf{Q}}^{D}_{\beta\alpha,\sigma'\sigma} = \left[\mathbf{G}^{a,0}(\epsilon)\Sigma^{a,0}_{\alpha}(\epsilon)\right]_{\sigma'\sigma} - \sum_{\pm} \frac{e^{-i(\epsilon\mp\epsilon_b)t}\left[\mathbf{P}^{*,a}(\pm\epsilon_b)\mathbf{\Sigma}^{a,0}_{\alpha}(\pm\epsilon_b)\right]_{\sigma'\sigma}}{\pm 2\epsilon_b(\pm\epsilon_b - \epsilon - \sigma' V_\beta + i0^+)}.$$

Based on $\tilde{\mathbf{A}}^{D}_{\beta}$ and $\tilde{\mathbf{Q}}^{D}_{\beta\alpha}$, we can extract the oscillating part of the current from $\tilde{J}_\alpha(t) = \tilde{J}^{\text{in}}_\alpha(t) + \tilde{J}^{\text{out}}_\alpha(t)$, where

$$\tilde{J}^{\text{in}}_\alpha(t) = 2\,\text{Re}\int \frac{d\epsilon}{2\pi}\text{Tr}\left[\tilde{\mathbf{A}}^{D}_{\alpha}(\epsilon,t)\mathbf{\Sigma}^{<,0}_{\alpha}(\epsilon)\sigma_z\right],$$

$$\tilde{J}^{\text{out}}_\alpha(t) = 2\,\text{Re}\sum_{\beta}\int \frac{d\epsilon}{2\pi}\text{Tr}\left[\tilde{\mathbf{A}}^{D}_{\beta}(t,\epsilon)\mathbf{\Sigma}^{<,0}_{\beta}(\epsilon)\tilde{\mathbf{Q}}^{D}_{\beta\alpha}(t,\epsilon)\sigma_z\right].$$

Substituting $\tilde{\mathbf{A}}_\beta$ and $\tilde{\mathbf{Q}}_{\beta\alpha}$ and applying the residue theorem, we derive the oscillating part of the current,

$$\tilde{J}^{D}_{\alpha,\sigma}(t) = 2\,\text{Re}\sum_{\beta,\sigma'\sigma'',\pm}\frac{e^{i(\mp 2\epsilon_b)t}}{4\epsilon_b^2}\mathbf{P}^{*,r}_{\sigma\sigma'}(\pm\epsilon_b)\left[\frac{\mathbf{\Sigma}^{<,0}_{\beta,\sigma'\sigma''}(\pm\epsilon_b)}{i(\pm 2\epsilon_b + \sigma'' V_\beta - i0^+)} - \frac{\mathbf{\Sigma}^{<,0}_{\beta,\sigma'\sigma''}(\mp\epsilon_b)}{i(\pm 2\epsilon_b - \sigma' V_\beta - i0^+)}\right]\left[\mathbf{P}^{*,a}(\mp\epsilon_0)\mathbf{\Sigma}^{a,0}_{\alpha}(\mp\epsilon_0)\sigma_z\right]_{\sigma''\sigma}. \quad (24)$$

In the derivation of the primary oscillating term from the equation above, we have omitted the time-dependent integral $\int d\epsilon e^{i\epsilon t}\ldots$. This simplification is justified as the contributions from different phases cancel each other out, leading to a net effect of zero on the long-term behavior. Additionally, we have disregarded the residue at the imaginary axis stemming from the Fermi distribution function. Since these residues are imaginary numbers, their contributions to the current decay exponentially with time, and thus, they do not influence the steady-state behavior and can be safely neglected. In Eq. (24), $\mathbf{\Sigma}^{<,0}$ is considered infinitesimally small because the lifetime of the bound states $\pm\epsilon_b$ is effectively infinite. When $V \simeq 2|\epsilon_b|$, we encounter a situation that leads to an indeterminate form of $\frac{0}{0}$, which corresponds to the maximum amplitude of the current oscillation.

In Fig. 5, the transient current J^D is plotted over time for different phase differences ϕ. The amplitude of the driving bias is set as $V(\phi) = 2|\epsilon_b(\phi)|$, which is dependent on ϕ, ensuring that the amplitudes of oscillation are maximal for the various ϕ values. The maximum values are approximately equal for ϕ and $2\pi - \phi$ due to the relationship $-\epsilon_b(\phi) = \epsilon_b(2\pi - \phi)$, as shown in Fig. 4. However, these values are distinct for different ϕ (represented by the three black lines or three red lines). With ϕ increasing from 0 to π, $|\epsilon_b|$ decreases monotonically, while the final steady current $J^D(t \to \infty)$ increases monotonically. As ϕ approaches π (for example, $\phi = \pi \pm 0.1\pi$), $\pm\epsilon_b$ is very small, and the oscillating terms are progressively merged by the nonequilibrium tunneling processes, as indicated by the dotted lines in Fig. 5.

When $\phi \to \pi$, $|\epsilon_b|$ diminishes to zero, but $J^D(t \to \infty)$ undergoes a sudden reversal from a maximum to a minimum, as depicted in Fig. 2(d). This phase transition is responsible for the nonequilibrium fractional Josephson effect [58]. Consequently, the transient current becomes singular at $\phi = \pi$. In Fig. 6, the transient current is plotted for $V(\phi) = 2|\epsilon_b(\phi)|$ and $\phi = \pi \pm 0.01\pi$. The current behavior is markedly different from that observed in Fig. 5, underscoring the singularity of the bound state at $\phi = \pi$. When V deviates from $2|\epsilon_b(\phi)|$, the oscillation amplitude is significantly reduced, and the persistent oscillation induced by the bound states gradually diminishes. This also explains the discrepancy in the oscillation amplitudes observed in Figs. 3(a) and 3(b).

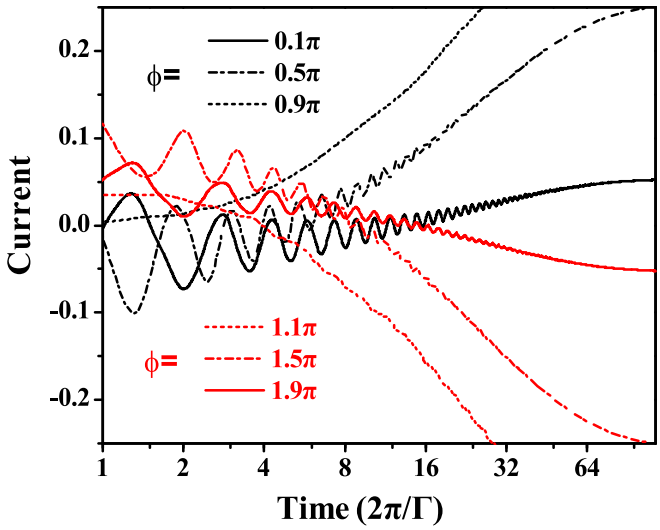

FIG. 5. Time dependence of transient current $J^D(t)$ when $V = 2|\epsilon_b|$ for different superconducting phase differences ϕ. The other parameters: $\Gamma = 0.8$.

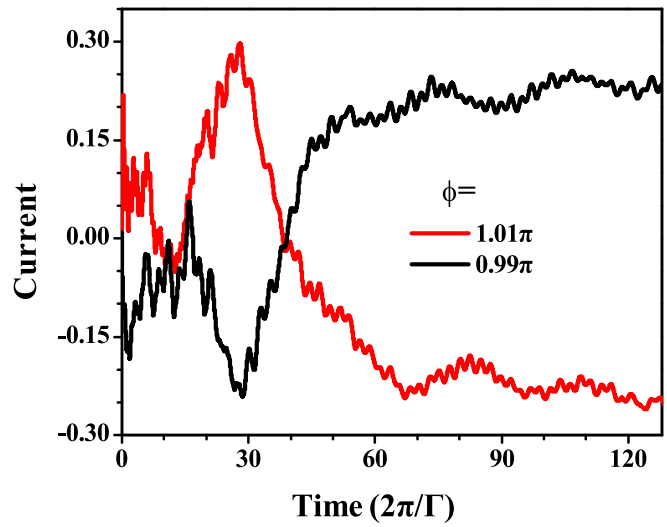

FIG. 6. Transient current near the critical point where $\phi = \pi$. The other parameters are the same as in Fig. 5.

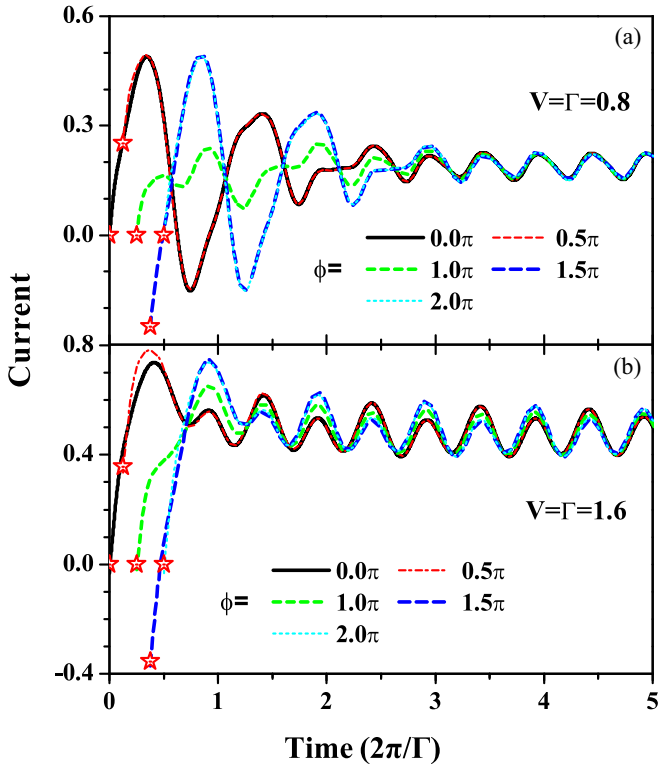

FIG. 7. Time dependence of transient current $J^U(t)$ driven by upwards step-like bias for different superconducting phase differences ϕ. (a) $V = \Gamma = 0.8$. (b) $V = \Gamma = 1.6$. In order to remove the phase shift ϕ of ac Josephson current, the time of $t = 0$ is shift to ϕ/ω (the red stars).

C. Turning-on transient current

In contrast, we present the "turning-on" transient current in this section. Upon the activation of the bias V at $t = 0$, the turning-on transient current J^U is triggered. In Fig. 7, we depict the temporal evolution of $J^U(t)$ for different superconducting phase differences ϕ. Before $t = 0$, the absence of bias sustains a steady dc Josephson current. Following $t = 0$, the dc current relaxes and ultimately achieves a new steady state, which is the ac Josephson current. Under the application of the dc bias V, the complex superconducting order parameter $\tilde{\Delta}_\alpha$ is transformed to $\tilde{\Delta}_\alpha e^{-2iV_\alpha t}$. Consequently, the superconducting phase difference ϕ evolves to become time dependent in a periodic manner, expressed as $\tilde{\phi} = \phi + 2Vt$. This results in a phase shift in the transient current J^U. To eliminate the phase shift of the ac Josephson current, we have adjusted the initial time from $t = 0$ to ϕ/ω in Fig. 7. By aligning all the repositioned initial currents, we are able to trace the trajectory of the DC Josephson current, which is illustrated in Fig. 2(d).

In Figs. 7(a) and 7(b), we select different biases V and different coupling strengths Γ. For ease of comparison, the initial dc current is marked by the red stars in Fig. 7. Since the initial time has been repositioned to ϕ/ω, the red stars clearly illustrate the entire period of phase dependence of the dc Josephson current. The initial current varies for different Γ, but all exhibit the same phase dependence $f(\sin\phi)$. When the bias is turned on, the single electrons are successfully scattered out of the superconducting gap with the aid of MARs rather than being trapped by bound states. As a result, the transient current rapidly stabilizes to the steady ac Josephson current. With the phase shift accommodated, the steady ac Josephson current for different ϕ now coincide precisely. Here, the current exhibits periodic oscillations with a period of $T = \pi/V$, as the bias V induces an effective periodic phase $\tilde{\phi} = \phi + 2Vt$. It is worth mentioning that periodic oscillations are observed in both the turning-on transient current J^U and the turning-off transient current J^D, yet they are fundamentally distinct. Indeed, as shown in Fig. 3, the oscillation period of J^D is dependent on the superconducting phase difference ϕ and is entirely independent of the bias V, whereas the oscillation period of J^U is determined by V. In the absence of bound states, the turning-on transient process is a conventional quantum transport phenomenon. Generally, the relaxation time $\tau \sim 2\pi/\Gamma$ that is dependent on the coupling strength Γ. From Fig. 7, we can estimate the relaxation time $\tau \simeq 8\pi/\Gamma$. This stands in stark contrast to the turning-off transient current J^D, where the relaxation time τ is significantly greater, by two orders of magnitude.

IV. CONCLUSIONS

In this paper, we use the Keldysh nonequilibrium Green's functions to explore the transient behaviors of Josephson junctions beyond the wide-band limit. We specifically analyze the "turning-off" and "turning-on" transients, which are driven by downwards and upwards step-like biases, respectively. Due to the distinct physical mechanisms that govern superconducting current in zero-bias and nonzero-bias scenarios, the quench dynamics of the "turning-on" and "turning-off" transient processes exhibit significant differences from each other. For the former case, aided by quasiparticle bound states within superconducting gap, the electrons are trapped and oscillate between $\pm\epsilon_b$. Consequently, the "turning-off" transient current oscillates at a frequency of $2|\epsilon_b|$ and approaches the final direct current (dc) state very slowly. The relaxation time is infinitely long, two orders of magnitude greater than $2\pi/\Gamma$. In contrast, the oscillating "turning-on" transient current, aided by MARs, rapidly reaches the steady alternating state with a finite relaxation time τ that is approximately $2\pi/\Gamma$, roughly equivalent to the relaxation time of the non-Josephson system. The infinite relaxation time associated with the "turning-off" transient current enables the experimental observation of quasiparticle trapping within the junction materials. Furthermore, the distinct quench dynamics observed during sudden "turning-on" and "turning-off" events are instrumental in detecting the intrinsic properties of quantum dots experimentally.

ACKNOWLEDGMENT

We acknowledge financial support by the National Natural Science Foundation of China (Grants No. 12174023 and No. 12034014).

APPENDIX A: UNPERTURBED GREEN'S FUNCTION $G^{r/a,0}$ WITH ZERO BIAS

We have made the assumption that the hopping elements $t_{k,\alpha}$ are independent of the momentum k within a broad range

of energies surrounding the Fermi level. Additionally, the density of states of the leads, denoted as ρ_α, is taken to be approximately constant within this energy range. Consequently, the normal line width function $\Gamma_\alpha = 2\pi\rho_\alpha|t_\alpha|^2$ is considered energy independent. The term Γ_α is commonly utilized to describe the coupling strength or the tunneling rate between the quantum dot (QD) and the superconducting leads. For simplicity, without loss of physical accuracy, we also set $\Gamma_L = \Gamma_R = \Gamma$.

In the absence of a bias, the retarded Green's function $\mathbf{G}^{r/a,0}$ is a function of the time difference $t - t'$ and can be expressed as follows:

$$\mathbf{G}^{r/a,0}(t-t') = \int \frac{d\epsilon}{2\pi} e^{-i\epsilon(t-t')}\mathbf{G}^{r/a,0}(\epsilon),$$

$$\mathbf{G}^{r/a,0}(\epsilon) = \left[\epsilon \pm i0^+ - \mathbf{H}_0 - \sum_\alpha \Sigma_\alpha^{r/a,0}(\epsilon)\right]^{-1}.$$

Here, $\mathbf{H}_0 = \begin{pmatrix}\epsilon_d & \\ & -\epsilon_d\end{pmatrix}$ represents the Hamiltonian of the isolated quantum dot. The retarded self-energy is given by

$$\mathbf{\Sigma}_\alpha^{r,0}(\epsilon) = \frac{i}{2}\frac{-\nu\Gamma}{\sqrt{\epsilon^2-\Delta^2}}\begin{pmatrix}\epsilon & -\tilde{\Delta}_\alpha^* \\ -\tilde{\Delta}_\alpha & \epsilon.\end{pmatrix}.$$

In this expression, $\nu = 1$ for $\epsilon > -\Delta$ and $\nu = -1$ otherwise. $\tilde{\Delta} = \Delta e^{i\phi_\alpha}$ denotes the complex superconducting order parameter. The advanced self-energy is $\mathbf{\Sigma}_\alpha^{a,0}(\epsilon) = [\mathbf{\Sigma}_\alpha^{r,0}(\epsilon)]^\dagger$. The lesser self-energy is defined as

$$\mathbf{\Sigma}_\alpha^{<,0}(\epsilon) = f_\alpha(\epsilon)\big(\mathbf{\Sigma}_\alpha^{a,0}(\epsilon) - \mathbf{\Sigma}_\alpha^{r,0}(\epsilon)\big).$$

When $|\epsilon| < \Delta$, $\mathbf{G}^{r/a,0}(\epsilon)$ possesses a pair of poles, which correspond to the levels of two bound states $\pm\epsilon_b$. Consequently, $\mathbf{G}^{r/a,0}(\epsilon)$ can also be expressed as

$$\mathbf{G}^{r/a,0}(\epsilon) = \frac{\mathbf{P}^*(\epsilon)}{(\epsilon \pm i0^+ - \epsilon_b)(\epsilon \pm i0^+ + \epsilon_b)}, \tag{A1}$$

where $\mathbf{P}^*$ is the adjoint matrix of $\mathbf{P}$, and $\mathbf{P} = [\mathbf{G}^{r/a,0}]^{-1}$, $\pm\epsilon_b$ are the roots of the determinant $|\mathbf{P}(\epsilon)|$.

APPENDIX B: UNPERTURBED GREEN'S FUNCTION $\mathbf{G}^{r,V}$ WITH STEADY BIAS V

When bias V is applied, the energy of both the quasiparticle and the Cooper pair is influenced. Consequently, the complex superconducting order parameter $\tilde{\Delta}_\alpha$ is modified to $\tilde{\Delta}_\alpha e^{-2iV_\alpha t}$. The phase difference $\phi = \phi_L - \phi_R$ between the two superconducting leads becomes periodically time dependent, expressed as $\tilde{\phi} = \phi + 2Vt$. The period T is determined by the relation $2\pi = 2VT$. The Green's function thus becomes a periodic function, which can be formulated as $\mathbf{G}^{r,V}(t,t') = \mathbf{G}^{r,V}(t+T,t'+T)$. It can be expanded using the following double-time Fourier transformation:

$$\mathbf{G}^{r,V}(t,t') = \sum_l e^{-il\omega t}\int\frac{d\epsilon}{2\pi}e^{-i\epsilon(t-t')}\mathbf{G}^{r,V}(\epsilon+l\omega,\epsilon).$$

For notational simplicity, we introduce the abbreviation $\mathbf{F}_{mn}(\epsilon) = \mathbf{F}(\epsilon + m\omega, \epsilon + n\omega)$ to represent the double-energy Green's function or self-energy function. Here, m and n can be considered as discrete matrix elements in the energy space. Employing the Dyson equation, we can express the Green's function as [16]

$$\begin{aligned}\mathbf{G}^{r,V}_{mn}(\epsilon) &= \delta_{mn}\mathbf{g}^r_m + \sum_{\alpha,l}\mathbf{g}^r_m\mathbf{\Sigma}^{r,V}_{\alpha,ml}\mathbf{G}^{r,V}_{ln} \\ &= \delta_{mn}\mathbf{g}^r_m + \sum_{\alpha,l}\mathbf{G}^{r,V}_{ml}\mathbf{\Sigma}^{r,V}_{\alpha,ln}\mathbf{g}^r_n.\end{aligned} \tag{B1}$$

Here, $\mathbf{g}^r_m = \mathbf{g}^r(\epsilon + m\omega)$ with $\mathbf{g}^r(\epsilon) = [\epsilon + i0^+ - H_0]^{-1}$ is the Green's function of the isolated quantum dot. We also introduce the abbreviation $\mathbf{F}_m(\epsilon) = \mathbf{F}(\epsilon + m\omega)$ to represent the single-energy Green's function or self-energy function.

Given that $V_L = V$ and $V_R = 0$, the self-energy of the right superconducting lead $\mathbf{\Sigma}^{r,V}_R$ equals $\mathbf{\Sigma}^{r,0}_R$. The biased self-energy of the left superconducting lead $\mathbf{\Sigma}^{r,V}_L$ is a tridiagonal matrix in the energy space, with elements

$$\mathbf{\Sigma}^{r,V}_{L,mn}(\epsilon) = \mathbf{\Sigma}^{r,0}_{L,m}(\epsilon_V)\cdot\mathbf{B}_{mn}, \tag{B2}$$

with

$$\mathbf{B}_{mn} = \begin{pmatrix}\delta_{m,n} & \delta_{m,n+1} \\ \delta_{m,n-1} & \delta_{m,n}\end{pmatrix},$$

$$\mathbf{\Sigma}^{r,0}_{L,m}(\epsilon_V) = \begin{bmatrix}\mathbf{\Sigma}^{r,0}_{L,m,11}(\epsilon - V) & \mathbf{\Sigma}^{r,0}_{L,m,12}(\epsilon - V) \\ \mathbf{\Sigma}^{r,0}_{L,m,21}(\epsilon + V) & \mathbf{\Sigma}^{r,0}_{L,m,22}(\epsilon + V)\end{bmatrix},$$

or

$$\mathbf{\Sigma}^{r,V}_{L,mn}(\epsilon) = \mathbf{B}_{mn}\cdot\mathbf{\Sigma}^{r,0}_{L,n}(\epsilon_V), \tag{B3}$$

with

$$\mathbf{B}_{mn} = \begin{pmatrix}\delta_{m,n} & \delta_{m-1,n} \\ \delta_{m+1,n} & \delta_{m,n}\end{pmatrix},$$

$$\mathbf{\Sigma}^{r}_{L,n}(\epsilon_V) = \begin{bmatrix}\mathbf{\Sigma}^{r,0}_{L,n,11}(\epsilon - V) & \mathbf{\Sigma}^{r,0}_{L,n,12}(\epsilon + V) \\ \mathbf{\Sigma}^{r,0}_{L,n,21}(\epsilon - V) & \mathbf{\Sigma}^{r,0}_{L,n,22}(\epsilon + V)\end{bmatrix}.$$

Here, "·" denotes matrix element multiplication. By substituting the tridiagonal self-energy into the Eq. (B1), we obtain the Nambu elements

$$\begin{aligned}\mathbf{G}^{r,V}_{\sigma\sigma} &= \left[\mathbf{R}^{-1}_\sigma - \sum_{\alpha,\beta}\mathbf{\Sigma}^{r,V}_{\alpha,\sigma\bar{\sigma}}\mathbf{R}_{\bar{\sigma}}\mathbf{\Sigma}^{r,V}_{\beta,\bar{\sigma}\sigma}\right]^{-1}, \\ \mathbf{G}^{r,V}_{\sigma\bar{\sigma}} &= \sum_\alpha \mathbf{G}^{r,V}_\sigma\mathbf{\Sigma}^{r,V}_{\alpha,\sigma\bar{\sigma}}\mathbf{R}_{\bar{\sigma}} = \sum_\alpha \mathbf{R}_\sigma\mathbf{\Sigma}^{r,V}_{\alpha,\sigma\bar{\sigma}}\mathbf{G}^{r,V}_{\bar{\sigma}},\end{aligned} \tag{B4}$$

with $\mathbf{R}_\sigma = [(\mathbf{g}^r_{\sigma\sigma})^{-1} - \sum_\alpha \mathbf{\Sigma}^{r,V}_{\alpha,\sigma\sigma}]^{-1}$. Here, σ and $\bar{\sigma}$ represent matrix elements in the spin space, with $\bar{\sigma}$ being the complementary set of σ. The matrix element of $\mathbf{R}_\sigma$ gradually diminishes with increasing size, allowing us to truncate the infinite matrix to a finite size and numerically solve for $\mathbf{G}^{r,V}$.

[1] E. Kleinherbers, P. Stegmann, A. Kurzmann, M. Geller, A. Lorke, and J. König, Pushing the limits in real-time measurements of quantum dynamics, Phys. Rev. Lett. **128**, 087701 (2022).

[2] U. Güngördü, R. Ruskov, S. Hoffman, K. Serniak, A. J. Kerman, and C. Tahan, Quantum dynamics of superconductor-quantum dot-superconductor Josephson junctions, arXiv:2402.10330v1.
[3] C.-P. Yang, Shih-I Chu, and S. Han, Possible realization of entanglement, logical gates, and quantum-information transfer with superconducting-quantum-interference-device qubits in cavity QED, Phys. Rev. A **67**, 042311 (2003).
[4] L. Hofstetter, S. Csonka, J. Nygård, and C. Schönenberger, Cooper pair splitter realized in a two-quantum-dot Y-junction, Nature (London) **461**, 960 (2009).
[5] L. G. Herrmann, F. Portier, P. Roche, A. L. Yeyati, T. Kontos, and C. Strunk, Carbon nanotubes as Cooper-pair beam splitters, Phys. Rev. Lett. **104**, 026801 (2010).
[6] J. Clarke and F. K. Wilhelm, Superconducting quantum bits, Nature (London) **453**, 1031 (2008).
[7] C. Padurariu and Y. V. Nazarov, Spin blockade qubit in a superconducting junction, Europhys. Lett. **100**, 57006 (2012).
[8] S. Park and A. L. Yeyati, Andreev spin qubits in multichannel Rashba nanowires, Phys. Rev. B **96**, 125416 (2017).
[9] L. Fu and C. L. Kane, Superconducting proximity effect and Majorana fermions at the surface of a topological insulator, Phys. Rev. Lett. **100**, 096407 (2008).
[10] R. Taranko, K. Wrześniewski, I. Weymann, and T. Domański, Transient effects in quantum dots contacted via topological superconductor, Phys. Rev. B **110**, 035413 (2024).
[11] M. Zgirski, L. Bretheau, Q. Le Masne, H. Pothier, D. Esteve, and C. Urbina, Evidence for long-lived quasiparticles trapped in superconducting point contacts, Phys. Rev. Lett. **106**, 257003 (2011).
[12] B. Tarasinski, D. Chevallier, J. A. Hutasoit, B. Baxevanis, and C. W. J. Beenakker, Quench dynamics of fermion-parity switches in a Josephson junction, Phys. Rev. B **92**, 144306 (2015).
[13] A. F. Andreev, Thermal conductivity of the intermediate state of superconductors, Sov. Phys. JETP **19**, 1228 (1964).
[14] D. Averin and A. Bardas, ac Josephson effect in a single quantum channel, Phys. Rev. Lett. **75**, 1831 (1995).
[15] D. Averin and A. Bardas, Adiabatic dynamics of superconducting quantum point contacts, Phys. Rev. B **53**, R1705 (1996).
[16] Q.-F. Sun, H. Guo, and J. Wang, Hamiltonian approach to the ac Josephson effect in superconducting-normal hybrid systems, Phys. Rev. B **65**, 075315 (2002).
[17] Q.-F. Sun, B.-G. Wang, J. Wang, and T.-H. Lin, Electron transport through a mesoscopic hybrid multiterminal resonant-tunneling system, Phys. Rev. B **61**, 4754 (2000).
[18] C. W. J. Beenakker, Josephson effect in a junction coupled to an electron reservoir, arXiv:2404.13976.
[19] I. O. Kulik, Macroscopic quantization and the proximity effect in S-N-S junctions, Sov. Phys. JETP **30**, 944 (1970).
[20] J. Bardeen and J. L. Johnson, Josephson current flow in pure superconducting-normal-superconducting junctions, Phys. Rev. B **5**, 72 (1972).
[21] J. Maciejko, J. Wang, and H. Guo, Time-dependent quantum transport far from equilibrium: An exact nonlinear response theory, Phys. Rev. B **74**, 085324 (2006).
[22] Y. Xing, Q.-F. Sun, and J. Wang, Response time of a normal-metal/superconductor hybrid system under a step-like pulse bias, Phys. Rev. B **75**, 125308 (2007).
[23] G. Stefanucci, E. Perfetto, and M. Cini, Time-dependent quantum transport with superconducting leads: A discrete-basis Kohn-Sham formulation and propagation scheme, Phys. Rev. B **81**, 115446 (2010).
[24] Y. Xing, B. Wang, and J. Wang, First-principles investigation of dynamical properties of molecular devices under a steplike pulse, Phys. Rev. B **82**, 205112 (2010).
[25] B. Wang, Y. Xing, L. Zhang, and J. Wang, Transient dynamics of molecular devices under a steplike pulse bias, Phys. Rev. B **81**, 121103(R) (2010).
[26] L. Zhang, Y. Xing, and J. Wang, First-principles investigation of transient dynamics of molecular devices, Phys. Rev. B **86**, 155438 (2012).
[27] R. S. Souto, A. Martín-Rodero, and A. L. Yeyati, Andreev bound states formation and quasiparticle trapping in quench dynamics revealed by time-dependent counting statistics, Phys. Rev. Lett. **117**, 267701 (2016).
[28] R. S. Souto, A. Martín-Rodero, and A. L. Yeyati, Quench dynamics in superconducting nanojunctions: Metastability and dynamical Yang-Lee zeros, Phys. Rev. B **96**, 165444 (2017).
[29] C.-Z. Yao, H.-L. Lai, and W.-M. Zhang, Quantum transport theory of hybrid superconducting systems, Phys. Rev. B **108**, 195402 (2023).
[30] D. Sun and J. Liu, Quench dynamics of the Josephson current in a topological Josephson junction, Phys. Rev. B **97**, 035311 (2018).
[31] G. Michałek, B. R. Bułka, T. Domański, and K. I. Wysokiński, Statistical correlations of currents flowing through a proximized quantum dot, Phys. Rev. B **101**, 235402 (2020).
[32] I. Snyman and Y. V. Nazarov, Keldysh action of a multiterminal time-dependent scatterer, Phys. Rev. B **77**, 165118 (2008).
[33] Z. Yu, L. Zhang, Y. Xing, and J. Wang, Investigation of transient heat current from first principles using complex absorbing potential, Phys. Rev. B **90**, 115428 (2014).
[34] C. J. Lindner, F. B. Kugler, V. Meden, and H. Schoeller, Renormalization group transport theory for open quantum systems: Charge fluctuations in multilevel quantum dots in and out of equilibrium, Phys. Rev. B **99**, 205142 (2019).
[35] K. Wrześniewski, B. Baran, R. Taranko, T. Domański, and I. Weymann, Quench dynamics of a correlated quantum dot sandwiched between normal-metal and superconducting leads, Phys. Rev. B **103**, 155420 (2021).
[36] R. Seoane Souto, A. E. Feiguin, A. Martín-Rodero, and A. L. Yeyati, Transient dynamics of a magnetic impurity coupled to superconducting electrodes: Exact numerics versus perturbation theory, Phys. Rev. B **104**, 214506 (2021).
[37] G. Cohen, E. Gull, D. R. Reichman, and A. J. Millis, Green's functions from real-time bold-line Monte Carlo calculations: Spectral properties of the nonequilibrium Anderson impurity model, Phys. Rev. Lett. **112**, 146802 (2014).
[38] I. Krivenko, J. Kleinhenz, G. Cohen, and E. Gull, Dynamics of Kondo voltage splitting after a quantum quench, Phys. Rev. B **100**, 201104(R) (2019).
[39] N. Dittmann, J. Splettstoesser, and N. Helbig, Nonadiabatic dynamics in single-electron tunneling devices with time-dependent density-functional theory, Phys. Rev. Lett. **120**, 157701 (2018).
[40] N. Dittmann, N. Helbig, and D. M. Kennes, Dynamics of the Anderson impurity model: Benchmarking a nonadiabatic

exchange-correlation potential in time-dependent density-functional theory, Phys. Rev. B **99**, 075417 (2019).
[41] P. Wang and S. Kehrein, Flow equation calculation of transient and steady-state currents in the Anderson impurity model, Phys. Rev. B **82**, 125124 (2010).
[42] R. Taranko and T. Domański, Buildup and transient oscillations of Andreev quasiparticles, Phys. Rev. B **98**, 075420 (2018).
[43] R. S. Souto, R. Avriller, A. L. Yeyati, and A. Martín-Rodero, Transient dynamics in interacting nanojunctions within self-consistent perturbation theory, New J. Phys. **20**, 083039 (2018).
[44] C. Caroli, R. Combescot, P. Nozières, and D. Saint-James, Direct calculation of the tunneling current, J. Phys. C: Solid State Phys. **4**, 916 (1971).
[45] C. Caroli, R. Combescot, D. Lederer, P. Nozières, and D. Saint-James, A direct calculation of the tunnelling current. II. Free electron description, J. Phys. C: Solid State Phys. **4**, 2598 (1971).
[46] C. Caroli, R. Combescot, P. Nozières, and D. Saint-James, A direct calculation of the tunnelling current: IV. Electron-phonon interaction effects, J. Phys. C: Solid State Phys. **5**, 21 (1972).
[47] R. Combescot, A direct calculation of the tunnelling current. III. Effect of localized impurity states in the barrier, J. Phys. C: Solid State Phys. **4**, 2611 (1971).
[48] M. Cini, Time-dependent approach to electron transport through junctions: General theory and simple applications, Phys. Rev. B **22**, 5887 (1980).
[49] B. Wang, J. Wang, and H. Guo, Current partition: A nonequilibrium Green's function approach, Phys. Rev. Lett. **82**, 398 (1999).
[50] N. S. Wingreen, A.-P. Jauho, and Y. Meir, Time-dependent transport through a mesoscopic structure, Phys. Rev. B **48**, 8487 (1993).
[51] A.-P. Jauho, N. S. Wingreen, and Y. Meir, Time-dependent transport in interacting and noninteracting resonant-tunneling systems, Phys. Rev. B **50**, 5528 (1994).
[52] Q.-F. Sun, J. Wang, and T.-H. Lin, Photon-assisted Andreev tunneling through a mesoscopic hybrid system, Phys. Rev. B **59**, 13126 (1999).
[53] M. H. Pedersen and M. Büttiker, Scattering theory of photon-assisted electron transport, Phys. Rev. B **58**, 12993 (1998).
[54] Y. Nambu, Quasi-particles and gauge invariance in the theory of superconductivity, Phys. Rev. **117**, 648 (1960).
[55] Q.-F. Sun, J. Wang, and T.-H. Lin, Resonant Andreev reflection in a normal-metal-quantum-dot-superconductor system, Phys. Rev. B **59**, 3831 (1999).
[56] Y. Xing, B. Wang, Y. Wei, B. Wang, and J. Wang, Spin pump in the presence of a superconducting lead, Phys. Rev. B **70**, 245324 (2004).
[57] A. Erdélyi, *Asymptotic Expansions* (Dover, New York, 1956).
[58] A. Lahiri, S.-J. Choi, and B. Trauzettel, Nonequilibrium fractional Josephson effect, Phys. Rev. Lett. **131**, 126301 (2023).